Evaluation of Implementing Mining Wastewater in Closed-Loop Pressure Retarded Osmosis

Ali Etemad Zadeh

A thesis
In the department of
Building, Civil, and Environmental Engineering

Presented in Partial Fulfillment of the Requirements
For the Degree of
Master of Applied Science (Civil Engineering)

At Concordia University
Montreal, Quebec, Canada

March 2022

CONCORDIA UNIVERSITY

SCHOOL OF GRADUATE STUDIES

This is to certify that the thesis is prepared

By: Ali Etemad Zadeh

Entitled: Evaluation of Implementing Mining Wastewater in Closed-Loop Pressure Retarded Osmosis

and submitted in partial fulfillment of the requirements for the degree of

Master of Applied Science (Civil Engineering)

complies with the regulations of the University and meets the accepted standards with respect to originality and quality.

Signed by the final examining committee:

_____ Chair
Dr. Fuzhan Nasiri

_____ BCEE Examiner
Dr. Fuzhan Nasiri

_____ BCEE Examiner
Dr. Chunjiang An

_____ Supervisor
Dr. Catherine N. Mulligan

Approved by

_____ Graduate Program Director
Dr. Mazdak Nik-Bakht

_____ Dean of Faculty
Dr. Ashutosh Bagchi

Date: _____ 2022

Abstract

Evaluation of Implementing Mining Wastewater in Closed-Loop Pressure Retarded Osmosis

Ali Etemad Zadeh

Pressure-Retarded Osmosis (PRO) is an osmotic process that is used to harvest energy from salinity gradients using a semi permeable membrane. The driving force in this system is the difference in produced osmotic pressure between feed and draw solutions. Water flows across the membrane from the feed side and mixes with the draw solution. The draw solution is pressurized at pressure less than the net driving force and depressurizes in a turbine to generate electricity. A thorough comparison between open-loop PRO (OLPRO) and closed-loop PRO (CLPRO) was made regarding their performance and costs. In this study, gold mining wastewater was investigated to be used as the feed solution in PRO and its potential was evaluated. Prior to the main process, this solution was pretreated using ultrafiltration (UF) and nanofiltration (NF) to separate large molecules, colloids, multivalent ions, heavy metals, etc. In each step the fouling components and mechanism were explained. NF permeate characterization showed high removal efficiency of the present ions and heavy metals separation. In PRO, a solution of $NH_3 - CO_2$ with concentration of 3M were used as the draw solution. The proposed system could generate power density of $15.0 \pm 0.4\ W/m^2$. In the last section, Thermal efficiency was calculated and improving this efficiency were discussed. Overall, the utilization of the mining wastewater as the feed solution in PRO showed good potential, though, foulant elements may still have a major impact on pre-treatment steps and harnessing the full potential of the PRO process.

Acknowledgements

Foremost, I would like to express my sincere gratitude to my advisor Prof. Catherine N. Mulligan for the continuous support of my study and research, for her patience, motivation, enthusiasm, and immense knowledge. Her guidance helped me in all the research and writing of this thesis.

I would like to thank the lab technician, Hong Guan, and my lab mates, Dr. Dileep Palakkeel Veetil and Dr. Liuqing Yang for helping me with the characterization analyses and my tests.

Contribution of Authors

Chapter 1:

Dr. Khaled Touati provided data for Table 1, illustrated Figures 2, revised and edited Sections 1.2 and 1.3.

Chapter 2:

Dr. Khaled Touati provided data for Table 2 and prepared the entire Section 2.6, and revised sections 2.2 to the end of 2.5.

Dr. Catherine N. Mulligan, Dr. Jeffery R. McCutcheon, and Dr. Md. Saifur Rahaman, reviewed and edited all the sections mentioned above.

A review paper was published recently, and it was used as part of the literature review (Sections 2.1 to the end of 2.6). Below, the paper is cited:

A. E. Zadeh, K. Touati, C. N. Mulligan, J. R. McCutcheon, Md. S. Rahaman, "Closed-loop pressure retarded osmosis draw solutions and their regeneration processes: A review," ***Renew. Sustain. Energy Rev.,*** **vol. 159, pp.112191, Feb. 2022.**

Table of Contents

List of Figures

List of Tables

List of Abbreviations

CAPEX	Capital expenditure	PRO	Pressure retarded osmosis
CLPRO	Closed-loop pressure retarded osmosis	RED	Reverse electrodialysis
CP	Concentration polarization	RO	Reverse osmosis
CTA	Cellulose triacetate	RSF	Reverse salt flux
ECP	External concentration polarization	SEC	Specific energy consumption
EGE	Enhanced geothermal energy	SG	Salinity gradient
ERD	Energy recovery device	SPS	Switchable polarity solvents
FO	Forward osmosis	SWRO	Seawater reverse osmosis
GHG	Greenhouse gas	TB	Turbine
HMIS	Hazardous material identification system	TDS	Total dissolved solid
IC	Ion chromatography	TFC	Thin-film composite
ICP	Internal concentration polarization	UF	Ultrafiltration
ICP-MS	inductively coupled plasma mass spectrometry	*Symbols*	
IEA	International energy agency	S	Membrane structural parameter
LCOE	Levelized cost of electricity	t	Membrane tortuosity
LCST	Least critical solution temperature	ε	Membrane porosity
LGH	Low-grade heat	D	Diffusion coefficient
MED	Multi-effect distillation	K	Solute resistivity
MF	Microfiltration	*Subscript*	
MD	Membrane distillation	C	Cold reservoir
MNP	Magnetic nanoparticles	D	Draw solution
MSF	Multi-stage flash	F	Feed solution
NF	Nanofiltration	H	Hot reservoir
OHE	Osmotic heat engine	s	Salt
OLPRO	Open-loop pressure retarded osmosis	RP	Regeneration process
ORC	Organic Rankin cycle	w	Water

Chapter 1: Introduction

1.1 Rationale

Advances in medical science and food production industries, and economic developments caused rapid population growth in the 20th century. In fact, Earth's population grew from 2 billion in 1927 to 6.3 billion in 2003, and it is expected to grow to 8.9 billion in 2050 [1]. Therefore, world energy consumption will rise almost 50% between 2018 and 2050 as a result of significant energy and electricity demand increase [2]. Therefore, humankind will face unprecedent challenges to provide energy. Due to discoveries and access to the fossil fuel resources such as oil, natural gas and coal, their consumption has increased drastically. In addition, end-use fuel consumption will increasingly shift toward electricity. These fuels have great contributions in electricity production in the world. According to the international energy agency (IEA), fossil fuel sources accounted for two-thirds of world's electricity generation in the year 2015 [2], as shown in Figure 1. However, fossil fuel consumption has two major problems. First, the resources are limited and non-renewable. Second, consuming these fuels emits greenhouse gases (GHG) such as CO_2 to the atmosphere which cause global warming and climate change. Moreover, industrial emissions such as power plants, as well as transportation vehicles have grave harmful effects on health. Burning fossil fuels leads to emitting dangerous substances such as carbon monoxide, nitrogen oxides, sulfur oxide, methane, and volatile organic compound [3]. Therefore, scientists and researchers tried to investigate new sources of energy that are renewable and clean with minimal impact on the environment to reduce the reliance on fossil fuels for providing energy demands.

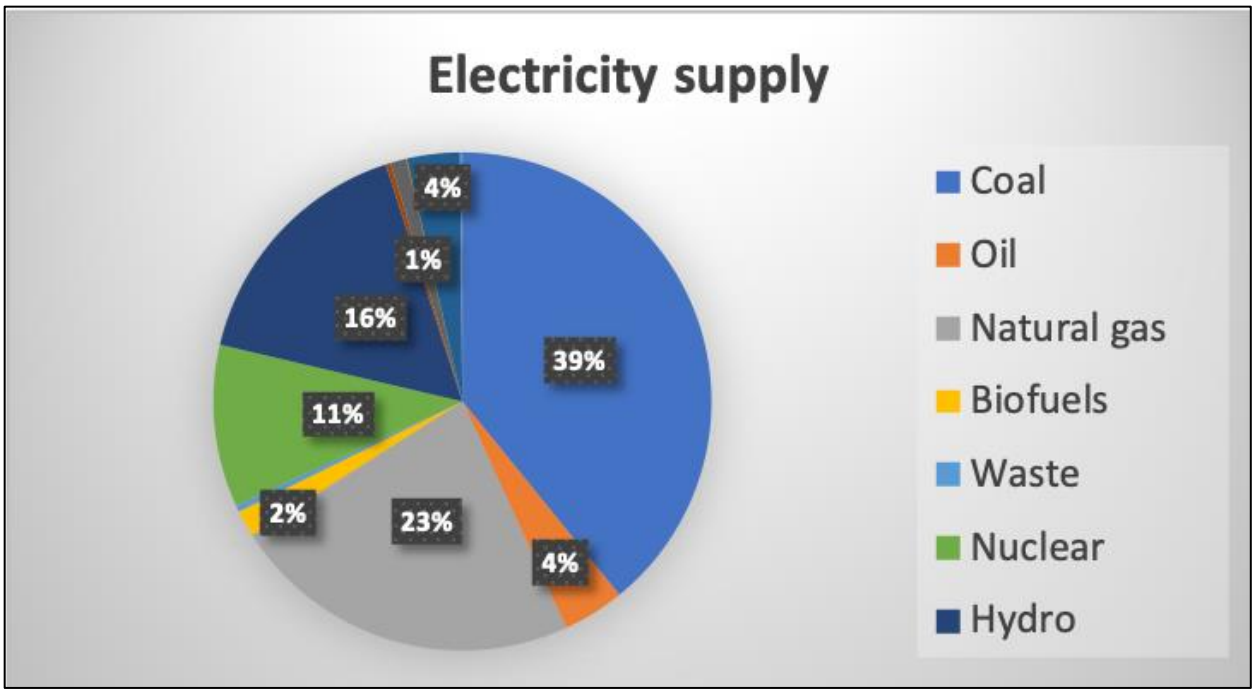

Figure 1: Schematic of electricity generation contribution [2]

1.2 Renewable Energy Overview

Renewable energy processes are necessary for the future of mankind. The share of renewable energy can grow from 15% in 2015 to 63% of the total primary energy supply in 2050 [4]. Such renewable energy growth in combination with higher energy efficiency can provide 94% of the emissions reduction that is needed to stay within the limits of the Paris Climate Agreement (keep the global temperature rise below 2 ℃ until the end of the current century) [4]. Currently, the most common and developed renewable energy sources are solar, wind, biomass, geothermal, and hydro [5]. Although these technologies have advantages over fossil fuels, there are some challenges regarding their utilization. For instance, in the solar process: (1) low efficiency, (2) high levelized cost of electricity (LCOE), (3) requirement of large quantities of land, (4) storage challenges and (5) availability [6]. Also, wind energy is facing some problems such as (1) high material costs like rotor blades, (2) noise and aesthetic pollution (3) harmful impacts on local wildlife, (4) wind forecasting models [7]. Application of geothermal and hydroelectric energies is

limited to certain areas and is not universal. Among renewable energy sources, biomass has the most contribution (72.3%) for providing energy worldwide with a potential capacity of 33,000 EJ [8]. However, the technologies for harvesting this energy are still not productive and cost-friendly. In fact, the production cost that ranged between 0.13 USD to 0.99 USD/L, is still high compared to the cost of electricity production (0.03 USD – 0.24 USD/kWh) [8].

1.3 Pressure Retarded Osmosis – A Promising Technology

Another potential source of clean energy is generated from salinity gradients (SG) [9,10]. SG energy can be harvested as electricity utilizing promising technologies such as pressure-retarded osmosis (PRO) and reversible electrodialysis (RED). PRO has been shown to be more efficient compared to RED for extracting power from SG [11]. In terms of energy conversion efficiency, defined as the ratio between the useful energy output and the energy input, SG shows better efficiency compared to other renewable energy sources as shown in Table 1, despite the various energy losses (Figure 2) that occur during the energy conversion process.

Table 1: Energy conversion efficiency of salinity gradient in comparison to other renewable energy sources

Renewable energy sources	Energy conversion efficiency (%)	Reference
Solar PV	22 – 50	[12]
Geothermal	10 – 17	[13]
Wind	35 – 45	[14]
Tidal	70 - 80	[15]
Hydro Power	60 – 90	[16]
Salinity Gradients	20 – 55	[17]

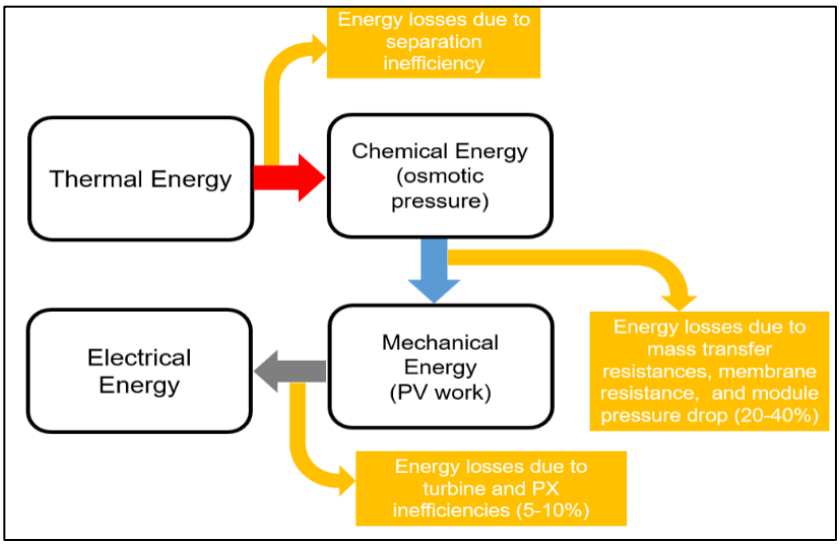

Figure 2: Energy losses during the conversion of SG to electrical energy [20]

1.4. Objectives of the study

- To determine the feasibility of implementing mining wastewater in CLPRO as the feed solution
- To evaluate the effectiveness of pre-treatment processes including ultrafiltration (UF) and nanofiltration (NF)
- To identify the fouling components
- To determine the amount of generated power density
- To determine the energy consumption of the PRO.

Chapter 2: Literature Review

2.1 Renewable Energy sources

Exploiting renewable energy sources is crucial for the future of humanity and saving the planet from the effects of climate change. Unlike fossil fuels, these energies are considered clean and sustainable which have various benefits for environment [80]. Solar energy is the most available source of energy and has many advantages. Annually, around 4 million Exajoules of solar energy is emitted to the earth of which about 1.25% (5×10^4 EJ) of that amount can be easily harvested [81]. There are two types of solar technologies: active and passive. In passive technologies, solar energy in the form of thermal or light is not converted to any other forms. For instance, collected solar heat can be used in heating homes during the winter season. On the other hand, active technologies convert collected radiation into electricity or heat using special equipment. These technologies can be categorized into two groups: solar thermal technology and photovoltaic technology. Photovoltaic technologies have drawn significant attention since the beginning of 21st century. In this system, semiconductors are employed to transfer sunlight directly into electricity. Energy that is harvested from wind currents is another source of clean and sustainable energy. This resource is widely available throughout the world and can contribute to electricity generation for domestic and industrial purposes. In order to convert wind energy into mechanical work, wind turbines are utilized. Wind turbines are divided into two groups: (1) horizontal axis type and (2) vertical axis type. Although the horizontal axis type is greatly developed and commercialized, the vertical type is more beneficial considering its footprint [82].

Geothermal energy is another type of renewable source which can be used to reduce CO_2 emissions. The superior advantage of geothermal energy over wind and solar is that this energy is a predictable and flexible resource which can have continuous electricity production 24 h per day

[83]. There are two kinds of geothermal energy; shallow geothermal and deep geothermal which are different in the depth of the well drilling. Among the technologies for harvesting this energy enhanced geothermal energy (EGE) is more efficient for electricity production [84]. The main advantage of this technology lies in extracting heat from tight rocks that have not been fractured naturally. By harnessing geothermal heat at different thermal levels in sequential processes (cascade utilization), the thermal efficiency of this system can be improved [85]. Currently, considering turbines inlet pressure and efficiency, the conversion of flowing steam thermal power into electricity is 20% [86]. Biomass energy is referred to as any type of energy which is achieved from non-fossil biological materials which have intrinsic chemical energy. It can be utilized for various purposes from cooking and heating to electricity generation and liquid or gaseous fuels [87]. Currently, most of the recent attention is on liquid transport fuels which are mainly ethanol from corn or sugarcane, and biodiesel from soy or palm oil [88]. Electricity production from biomass can happen through direct combustion of biomass, biogas and pyrolysis oil. Gasification processes are used to convert biomass to combustible gas or biogas which employing it in gas turbine will generate electricity. Pyrolysis is the anaerobic thermal decomposition of biomass which is categorized into three different types: slow, fast and flash pyrolysis. Fast pyrolysis happens at moderate temperature and high heating rate not as much as flash which favors the production of bio-oil. This method out benefits the other ones due to higher energy efficiency and lower capital costs [89]. Also, bio-oil is more convenient in storage and transport compared to other pyrolysis products. Hydropower is one of the renewable sources for electricity production. In this process, natural moving waters passing through a hydro-turbine to generate electricity. Recently, this technology became more popular due to its continuous supply, relatively low costs, and immediate power provision to the grids [90].

2.2 Pressure Retarded Osmosis Overview

In PRO, water permeates spontaneously across a semi-permeable membrane from the low-saline feed solution (low osmotic pressure) into the pressurized draw side with high salinity (high osmotic pressure). The driving force in this system is the difference in osmotic pressure across the membrane which is higher than the applied pressure (ΔP) on the draw side. As the water permeates through the membrane, the draw solution becomes diluted, while the feed solution will become concentrated. Thus, the effective draw solution across the membrane decreases, and eventually, system will be in equilibrium state. By depressurizing the permeate through a turbine, power will be generated. There are two types of standalone PRO based on their configuration: open-loop (OLPRO) and closed-loop (CLPRO). An open-loop system is based on the mixing of relatively fresh water with saline water, where both outlet streams are discharged. On the other hand, in the CLPRO configuration, both streams exiting the PRO membrane modules, go to the regeneration process and then, are circulated back into the process. Although this process seems promising for future applications, it has some drawbacks. Reverse salt flux (RSF) from the draw side toward the feed side will cause concentration polarization (CP), consisting of internal concentration polarization (ICP) and external concentration polarization (ECP).

2.3 Closed-loop versus Open-loop Pressure Retarded Osmosis

CLPRO and OLPRO, both illustrated in Figure 3, are the two main configurations for hydraulic pressure-based salinity gradient power. Despite some common elements and overall operating principles, the two designs present substantial differences in terms of operation, draw solution types and sources, power production potential, economics, and environmental impact. In OLPRO, natural saline sources are generally the primary origin of the draw solutions, such as seawater and hypersaline lakes [10,18,19]. For the feed solution source, the majority of studies

have considered freshwater [10,20], wastewater [17,21], or even seawater [18] as a low concentration feed. OLPRO can be located where these feed and draw solutions are both abundant and within close proximity to each other.

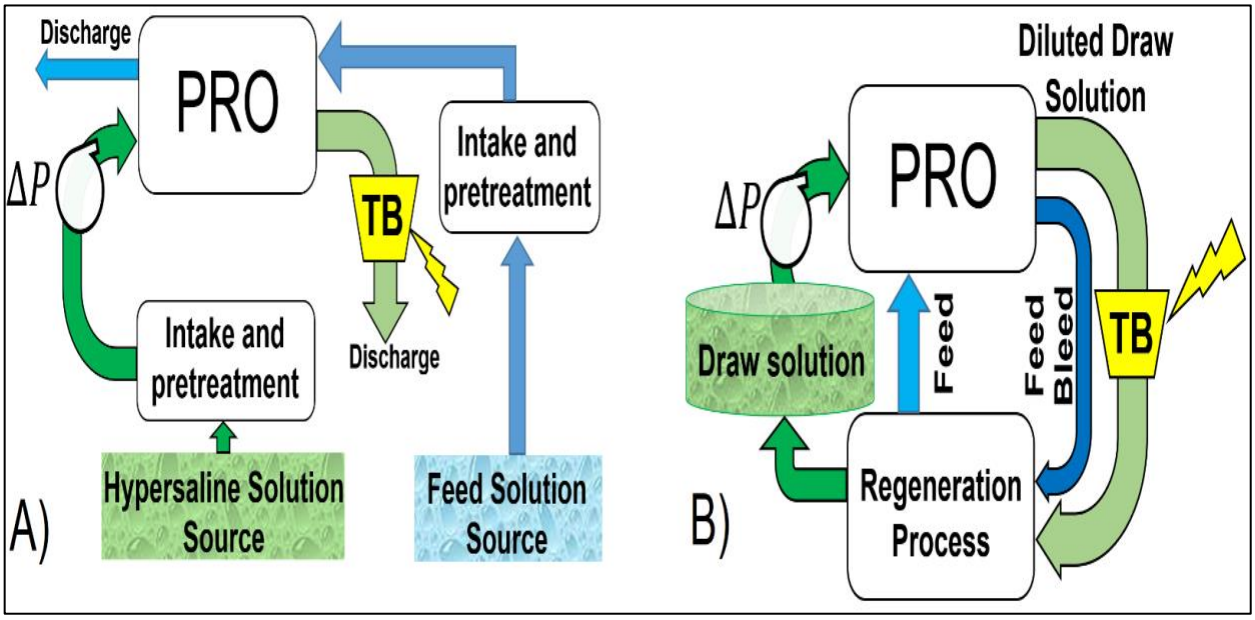

Figure 3: Schematic of (A) OLPRO and (B) CLPRO for energy harvesting. TB is the turbine.

In CLPRO, the feed and draw solution are continuously regenerated using heat or other processes. CLPRO requires this energy to re-concentrate the draw solution and remove water, which can then both be remixed in a conventional PRO process. Unlike with OLPRO, the system designers can choose precisely which draw solution they want to use, giving flexibility in design based on available energy sources at a particular location. In OLPRO, not only pre-treating both feed and draw solutions, but also the energy consumption due to transporting streams from natural or industrial sources to the PRO plant highly affects cost. Also, the risk of membrane fouling is higher in an open-loop system which leads to a higher membrane cost. The OLPRO plant location is limited to places close to the inlet streams and thus cannot be applied far from these sources. However, CLPRO can operate with more flexibility and with minimal footprint, except for the osmotic heat engines which must be close to the low-grade heat (LGH) sources to recover the

diluted draw solution. In CLPRO, there is no discharge and it is completely environmentally friendly. However, in OLPRO, the outlet streams are discharged, especially when natural sources are used as the streams. Overall, CLPRO seems to be more flexible and practical, and a better option for the applicability of PRO. Table 2 briefly describes the general performance of the two PRO configurations. To make it feasible, two parameters should be well-controlled and minutely selected in CLPRO: the draw solution and the regeneration process.

Table 2: Advantages, disadvantages and challenges for CLPRO and OLPRO [95]

	Energy production	Operation	Cost	Environmental impact
CLPRO	Advantages • Operates at higher osmotic and hydraulic pressures for higher power density • Can generate more power per module and in a smaller system footprint than other PRO systems Disadvantages • Draw solution regeneration requires thermal or equivalent energy source • Draw recovery adds an energy efficiency loss • Overall low Carnot efficiency	Advantages: • Can operate wherever waste heat is available • No liquid waste or intake Challenges: • Relies on effective capture of waste heat for draw solution regeneration • Must have components that can handle operating pressures to maximize power production and justify installation • System components must be tolerant to the draw solution chemistry • Draw solute leakage to the feed must be recovered to ensure closed loop operation	Advantages: • High power density can lead to smaller systems with smaller footprint • Draw solution is 100% recycled. The solution does not need to be replaced, unless it ages or spoils • Better revenue from higher power density system using heat that would otherwise be discarded Challenges: • Specialty, high pressure and chemically tolerant components may be needed to accommodate higher pressures that make CLPRO relevant • Exotic draw solutes may constitute an expensive up-front cost • Draw solution regeneration process adds CAPEX	Benefits: • Capture of waste heat that would otherwise be discarded • CO_2 life-cycle offsets from conventional electricity generation • No waste streams Challenges: • Membrane and draw solution life-cycle must be considered based on lifetime of the plant
OLPRO	Advantages • Draw solution does not require energy • Disposal, rather than recycling, of solution mixture Disadvantages • Generates limited power because of osmotic and hydraulic pressure limitations to all but the most naturally occurring brine solutions (and these natural brines often occur in arid places with little freshwater) • Net power production is limited by power consumption for extensive pretreatment and pumping costs for the intake and outfall	Advantages: • Naturally occurring draw solution • Extensive experience with intakes and outfalls of saline and freshwater sources Challenges: • Natural water requires extensive pre-treatment to prevent fouling, leading to complex systems with more maintenance and failure points • Geographically limited to locations where freshwater and saline water mix naturally • Permitting challenges for intakes and outfalls	Advantages: • Naturally occurring salinity gradients offer basic energy source for “free” • Lower operating pressures enable use of off-the-shelf components for systems Challenges: • Pretreatment system incurs significant CAPEX and OPEX costs and power losses • OLPRO systems have yet to yield net positive power production • Low energy generation potential makes ROI targets challenging to meet.	Benefits: • Capture of energy of mixing that would otherwise be lost • CO_2 life-cycle offsets from conventional electricity generation • May offer a means of reconstituting inland saline seas Challenges: • Intake and outfall environmental impacts • Disruption of delicate estuary environments • Requires use of freshwater or lower salinity waters in arid regions • Pretreatment chemical use and disposal life cycle • Membrane life cycle costs

2.4 Draw solutes

2.4.1 Criteria for draw solute selection

The draw solution is a crucial parameter in the PRO process since it controls several factors, such as the driving force and salt leakage which affects the process performance directly, and consequently, the generated power density. Achilli et al. [22] proposed a procedure for the selection of suitable inorganic draw solutions, including a desktop screening process, followed by a laboratory and modeling analysis. According to his work, a suitable draw solute must have the following criteria: (1) soluble in water, (2) be solid at ambient temperature and pressure, (3) not toxic, nor a code below 2 within the Hazardous Materials Identification System (HMIS), with 0 denoting minimal danger and 4 representing a severe or lethal hazard, (4) produces an osmotic pressure more than 1 MPa (145 psi) at saturation concentration, and (5) has a specific cost, i.e., the cost of solutes to produce one liter of draw solution which can generate 2.6 MPa (406 psi) of osmotic pressure, and less than 10 USD/L. However, requiring a non-toxic draw solution, especially for a CLPRO, is not a requirement as it is not used for human or animal consumption. As for the cost, this value was not suggested based on existing processes or developed cost estimation. Also, even if the draw solution price is relatively high, it might have a slight impact on the overall energy cost especially in the case of CLPRO when the solute is recoverable.

Moreover, there are some other important criteria that should be taken into consideration such as: (a) solute solubility, (b) solute flux tolerance, (c) viscosity, (d) recoverability of the draw solution, (e) solute diffusivity, and (f) compatibility with the membrane. High solubility has a direct relationship with the generated osmotic pressure. The trans-membrane osmotic pressure difference is the driving force in PRO. Therefore, higher solubility leads to better osmotic performance and higher water flux (J_w). Also, the solute must have minimal RSF (J_s). As not only

diffusing solutes from the draw side into the feed side leads to reduction in effective driving force across the membrane, the trace of the draw solute in the feed side also may exacerbate fouling. Moreover, the draw solution's viscosity at high concentrations is an important factor. High viscosity may affect the hydrodynamics at the surface of the membrane (low mass transfer) due to the laminar flow, lead to more energy consumption for pumping, severe external concentration polarization (ECP) in the draw side, and reduction in particle dissociation that lowers water flux. In terms of cost effectiveness, the diluted draw solution must be re-concentrated at a competitive cost and energy-efficient way. The regeneration stage is the most crucial part of the system's total energy consumption. The extracted energy from the process must out-balance the required energy in the regeneration system, and it is the main factor in indicating whether the process is applicable or not.

2.4.2 Categorization of draw solutes described in the literature

Draw solutes can be categorized by their physio-chemical properties, and many research groups have worked on optimizing draw solutions in PRO. Table 3 demonstrates a list of the main types of draw solutions investigated in the literature for CLPRO application, categorized by their generated osmotic pressure and power density, the method of their recovery, and their advantages and drawbacks as the draw solution in PRO. In the following sections, these draw solutes are defined, and their advantages and drawbacks are discussed. Also, their performance under the closed-loop system is critically discussed. The draw solutes in the literature are categorized into gaseous and volatile compounds, inorganic, organic, and functionalized nanoparticles.

Table 3: Summary of potential draw solutes described in the literature in stand-alone closed-loop PRO systems

Draw solutes	Osmotic pressure /Concentration	Water flux /Power density	Regeneration	Advantages	Drawbacks	Ref
KCit **CaAc** **KOxa** **KAc** **NH_4Ac** **NH_4C** **NH_4F** **KF** **NaGly** **NaP** **CaP** **NaCl** **NH_4HCO_3**	42 bar/0.62 M 42 bar/1.22 M 42 bar/0.55 M 42 bar/0.97 M 42 bar/1.32 M 42 bar/0.58 M 42 bar/0.91 M 42 bar/0.99 M 42 bar/1.07 M 42 bar/1.01 M 42 bar/0.87 M 42 bar/0.93 M 42 bar/1.03 M	11.12 W/m^2 12.03 W/m^2 12.45 W/m^2 12.70 W/m^2 13.06 W/m^2 13.55 W/m^2 13.70 W/m^2 13.85 W/m^2 14.36 W/m^2 14.56 W/m^2 14.67 W/m^2 10.21 W/m^2 9.57 W/m^2	MD MD MD MD Thermolytic Thermolytic Thermolytic MD MD MD MD	* High osmotic pressure, water flux, and power density * Low RSF	* High viscosity at high concentrations	[23]
$Na_5[Fe(C_6H_4O_7)_2]$	58 bar/1 M	48.6 LMH/16.2 W/m^2 (applied pressure: 12 bar)	Precipitation	High osmotic pressure and power density at low concentrations	High viscosity at high concentrations	[24]
NaCl	1.5 M (20 ℃) 1.5 M (40 ℃)	8.8 ± 1.0 W/m^2 18.0 ± 2.3 W/m^2	Thermal	Higher water flux and power density due to temperature increase	Increase in RSF	[25]
LiCl − methanol	2 M 3 M	37.8 LMH/31.3 W/m^2 47.1 LMH/72.1 W/m^2 (theoretical)	MD	More efficient regeneration, better performance	* Difficult to incorporate with OHE Due to high volatility of methanol * Methanol is more expensive than water	[26]
$NH_3 - CO_2$	191.6 bar/4.6 M (applied pressure: 101.3 bar)	170 W/m^2 (theoretical)	Distillation	High solubility, low molecular weight, high diffusivity, completely removeable (60 ℃), produces high osmotic pressure	High RSF, volatile	[27]
$CaCl_2$ **HCOONa** **KBr** **LiBr** **LiCl** **$MgCl_2$** **$Na(C_2H_5COO)$** **NaCl**	174 bar/1.6 M 174 bar/4.1 M 174 bar/3.2 M 174 bar/2.2 M 174 bar/2.6 M 174 bar/1.5 M 174 bar/4.1 M 174 bar/3.0 M	30 LMH/17.6 W/m^2 9.5 LMH/11.2 W/m^2	MD	High solubility, High pressure osmosis	High RSF for inorganic draw solutes	[28]
NaCl **$MgCl_2$** **$MgSO_4$**	1 M 0.67 M	14.88 W/m^2 10.2 W/m^2	MD	High solubility, High pressure osmosis	High RSF	[29]
NaCl	4 mol/kg	-	MD	-	-	[30]
NaCl	3 M	87 W/m^2	LGH	High power density	-	[31]

2.4.2.1 Gases and volatile compounds

McGinnis et al. [27] assessed theoretically osmotic heat engines (OHEs) and their potential for power generation and introduced ammonium-carbon dioxide as a novel draw solute for PRO. $NH_3 - CO_2$ is highly soluble in water, thus producing high osmotic pressure. However, it has a high diffusion constant, causing high RSF and severe water flux decline. Ammonia is a nutrient and may promote biofouling on the feed side of the membrane [32]. McGinnis et al. [27] stated that this draw solute at 4.6 molar which generates 199.6 bars of osmotic pressure, can theoretically produce 170 W/m^2 under a 101.3 bar applied pressure. Furthermore, by increasing the crossflow velocity which leads to reduction in ECP, or using a higher applied pressure, higher power densities are achievable. Based on modelling of OHE with increased crossflow velocities (5 m/s in a 0.05 cm high flow channel), the author concluded that the power density would be increased by almost 61% (from 170 W/m^2 to 274 W/m^2) compared to the system used in their study (0.46 m/s in a 0.3 cm high channel). In the matter of higher applied pressure, increasing the applied pressure from 101.3 bars (100 atm) to 202.6 (200 atm) could result in 47% more power density. However, higher crossflow velocities and applied pressures will result in higher energy consumption and high-performance equipment. Therefore, capital and operation costs should be optimized in the process design. Although, increasing the draw solution concentration can result in higher PRO performance, it increases the RSF which leads to lowering the effective driving force in the system and increasing energy consumption in the regeneration process. This draw solution can be separated efficiently using waste heat. Unavailability of commercial membranes that are sturdy enough to handle high applied pressure (more than 50 atm), is still a critical issue. The availability of membranes with higher mechanical strength and salt rejection plays a vital role in process viability.

2.4.2.2 Inorganic draw solutes

The most common inorganic draw solutes are monovalent salts, and more precisely, NaCl. These salts have some advantages such as: (a) they can produce a relatively high osmotic pressure with high water flux, (b) at high concentrations they have low viscosity, (c) they have high diffusion coefficients due to their small size, reducing the effect of ICP, (d) they can be separated easily through thermal processes, and (e) they are inexpensive and available in large quantities. However, their small size leads to high RSF, which causes flux reduction and lowers PRO performance. Also, their reverse flux can promote organic fouling on the feed side [32]. Moreover, multivalent salts outperform monovalent ones. These ions have less RSF due to their larger hydrated radius and produce higher osmotic pressures with the same molar concentrations [22].

Straub et al. [30] investigated 3 M NaCl as the draw solute and claimed an unprecedent power density of 59.7 W/m^2, with an impressive water flux of 44.5 LMH using an HTI TFC membrane, which withstood 48.3 bars of hydraulic pressure. Based on osmotic pressures simulated by OLI software, they predicted higher power densities that can be achieved using this draw solution. It is illustrated that with the availability of more robust commercial membranes, under 100 bars applied pressure, the power density could increase to 75 bars. This study showed flow channel and spacer design, and suitable membrane availability allow higher applied pressure which results in higher power densities. Anastasio et al. [25] investigated the impact of draw solution (NaCl) temperature on power density under conditions similar to OHE. As temperature increases, the water flux increased due to enhanced mass transfer, which results in higher power density. At 1.5 M NaCl, by increasing temperature from 20 ℃ to 40 ℃, the resulting power density increases from 8.8 ± 1.0 W/m^2 to 18 ± 2.3 W/m^2 at 20.7 bars, However, elevated temperature will lead to increased salt flux which was caused by increased salt diffusivity and reduced dilutive ECP,

resulting in water flux decline and ICP promotion [33]. Although, a higher temperature leads to better PRO performance, increased RSF will result in higher required energy in the re-concentration of the diluted draw solution which decreases process energy efficiency. This required energy is provided by available waste heat. This heat might be in large amounts but harnessing and using it in the regeneration unit comes with costs. Therefore, a trade-off should be made in this case.

Hickenbottom et al. [34] also used a NaCl solution as the draw solution. They studied different FO membranes which were commercially available and evaluated their performance in PRO and assessed the effects of feed and draw stream spacers and cross-flow velocities on generated power density. Three polyamide-based thin-film composites (TFC), and one HTI cellulose triacetate (CTA) were used in the experiments. According to the results, HTI TFC showed the highest mechanical strength, Power density (15.5 W/m^2 under 35 bars), selectivity, and lowest salt diffusion among the tested membrane. This membrane was tested under different applied pressures. Although, it can withstand pressures up to 48 bars (~ 700 psi), under pressures more than 35 bars (~ 500 psi), the support layer becomes thinner which causes porosity reduction and tortuosity increase. This phenomenon leads to a higher membrane parameter structure which promotes ICP and power density reduction. Three types of spacers were investigated in this study: 20-channel tricot, 35-channel tricot, and extruder mesh spacer, with different orientations. The highest power density achieved when the feed spacer was a two 20-channel tricot that was positioned at 45° to the feed flow. The reason behind it is due to increased mass transfer at the membrane interface, and consequently, decreasing the concentration polarization. For the draw side, an increase of 76% in power density was observed when one 20-channel tricot spacer and one extruded mesh spacer were used compared to two extruded mesh spacers. It is concluded that

by using these two configurations for feed and draw sides, the power density of 22.6 W/m^2 can be achievable in comparison with when there are no spacers under 35 bars applied pressure. Moreover, they concluded that the feed cross-flow velocity has more impact on power density than the draw side. Mass transfer in the feed side, affects process performance more. By increasing the feed and draw solutions cross-flow velocity from 2.6 cm/s to 13 cm/s, the power density increased 48% and 36%, respectively.

Shaulsky et al. [26] investigated an organic solvent, methanol, and compared its performance to water for a LiCl draw solute. LiCl is highly soluble in polar solvents due to the existence of strong ion-dipole force between Li^+ and polar solvents. It is depicted that the membrane solvent permeability for water (37.78 LMH) is ~55% more (26.25 LMH for LiCl-methanol) when the draw solution concentration is 1 M. Higher polarity of water molecules cause higher permeability due to more sorption of these molecules on the membrane's polyamide layer. On the other hand, the solute permeability in methanol is almost half of the water solution. It can be deduced that Li^+ and Cl^- ions form a larger solvated ion size in methanol, so, the solute flux is less. Moreover, membrane structural parameter (*S*) in the LiCl-methanol case is lower. The reason for this phenomenon is methanol surface tension is higher than water. Therefore, the support layer of the membrane will be wetted better resulting in lower *S,* and less severe ICP. Although LiCl-methanol has a lower water flux than LiCl-water, the ratio of J_w/J_s is higher for methanol solutions, thus, it performed more efficiently than water in terms of reverse diffusion. The predicted power density for LiCl-methanol solution at 3 M is 72.1 W/m^2 which makes it a potent potential draw solution for PRO. To achieve this power density, an applied pressure of 114 bars is needed which with the currently available membranes is not possible. Methanol has a lower enthalpy of evaporation than water. In terms of thermal separation and recovery, methanol is more

efficient. However, methanol is highly volatile, and it is hard to incorporate with OHEs, and it is more expensive than water.

Hickenbottom et al. [28] assessed alternative inorganic and organic ionic salts for an optimized closed-loop OHE using MD as the regeneration process. The experimented draw solutions are listed in Table 3. Solutions with different concentrations, which produce 174 bars of osmotic pressure were used as the draw solution. Among the selected draw solutes, HCOONa had the highest (30 LMH and 17.6 W/m^2), and $Na(C_2H_5COO)$ had the lowest (9.5 LMH and 11.2 W/m^2) water flux and generated power density. The difference in water fluxes is caused by ICP (the same membrane was used in all experiments) which is related to different solute diffusivity and salt permeability (B). Analyzing RSF, HCOONa had the lowest solute flux (11.8 gMH) due to its large hydration diameter affecting salt permeability. Thermal efficiency (the ratio of water flux to total heat flux), is another criterion investigated by author. It was determined that KBr had the highest thermal efficiency (94%), and $Na(C_2H_5COO)$ had the lowest one, due to its high heat capacity and low MD water flux. Working fluids with high thermal efficiency are the most suitable ones for OHE. The total electricity generation costs were calculated for each draw solution. The total electricity costs for $CaCl_2$ was the lowest, 1.65 USD per kWh. The MD membrane cost has the largest contribution to the system cost. Since, $CaCl_2$ had low RSF, the MD membrane cost was low. Also, it had highest net energy production, the lowest system costs, the second highest power density, and the second highest MD flux. Considering specific cost, RSF, power density, MD water flux and thermal efficiency, net power generation, and electricity generation cost, the author suggested that $CaCl_2$ is the best draw solute. Still, compared to other sources of renewable energies, energy generation cost for OHE is high. The introduction of more robust and selective membranes

for PRO could be helpful in harnessing the full potential of this draw solution and resulting in reasonable electricity generation cost.

Gong et al. [29] investigated the transport of ions during PRO in order to find better draw solutes for an OHE. Three inorganic salts were selected for this study: NaCl, $MgCl_2$, and $MgSO_4$. Apparently, ions with larger hydrated ion diameter have a lower solute permeability because more water molecules surround ions with higher charge density, which leads to higher polarization. Smaller ions with higher valence have higher charge density, and consequently, higher larger hydration diameter. According to their results, $MgSO_4$ had the lowest power density due to its lower osmotic coefficient (φ) compared to the other two, φ for $MgSO_4$ at 1 M is 0.525 which is much lower than 1.004 ($MgCl_2$) and 0.926 (NaCl) at 0.67 M [40]. Moreover, this draw solute showed poor mass transfer due to its higher viscosity and lower diffusion coefficient, resulting in more ECP on the draw side. $MgCl_2$ generated more power density compared to NaCl because of its larger hydration diameter, which increases the membrane selectivity and reduces the effect of ICP. Overall, draw solutes with smaller hydrated ion sizes have higher water fluxes and diffusion coefficients, leading to an increased RSF, which promotes ICP. On the other hand, larger ions have lower RSF, but higher viscosity at the same concentration, promotes ECP. Therefore, trade-offs of these parameters should be considered to select the optimized draw solution with the best performance.

Moon et al. [31] investigated a new type of membrane in OHE for comparing its performance with other renewable technologies based on LCOE. Direct fluorination (converting C-H bonds to C-F bonds within a polymer) is used in a one-step gas-phase reaction to enhance the surface characteristics of the support layer. Fluorination of PBO-TFC increased the membrane's hydrophilicity resulting in better rejection (R value) for the selective layer (increased from 90.7%

to 95.9 $\pm$ 1.7 %). Although the fluorination resulted in increased A and B values compared to other membranes, the significantly low structural parameter (S = 142 μm) is promising for better PRO performance. Using 3 M $NaCl_{aq}$, PBO-TFC-F5 showed way more transmembrane water flux (116.2 – 147.2 LMH) than un-fluorinated PBO-TFC (33.9 – 86.0 LMH). Obviously, the reduced ICP is the reason behind this result due to super hydrophilicity (high R) nature and crumpled selective layer (high A) of PBO-TFC-F5. Also, considering that the mechanical strength of PBO-TFC cannot be operated at pressures above 21 bars, implementing 1 M and 3 M NaCl draw solutions, PBO-TFC-F5 generated 17.6 W/m^{-2} and 87.2 W/m^{-2} power density under hydraulic pressure of 18 and 27 bars, respectively. For the first time, a research group claimed this high power density in CLPRO, which outperforms HTI-TFC membranes (6-8 times better performance) under the same experimental conditions. Furthermore, using feed solutions with higher concentrations (industrial applications) from DI water to 0.5 M NaCl (seawater), increases the power density ratio of PBO-TFC-F5 to HTI-TFC even more. This modified membrane has a much lower S value of the support layer compared to commercially available HTI-TFC, and consequently, much less severe ICP happens in its support layer. This study shows promising results for feasibility and practical implementation of PRO at industrial scale.

2.4.2.3 Organic draw solutes

Organic draw solutes have two main advantages compared to inorganic salts: (1) the former's hydrated ion sizes are larger than the inorganic salts, resulting in better membrane selectivity. Therefore, their RSF is much lower, and less water flux decline happens during the operation. Additionally, due to lower RSF the required energy for feed solution regeneration, and replenishment costs are lower as well. (2) organic draw solutes can be engineered and tailored to change their properties and increase their PRO-related performance. However, their larger size

leads to lower diffusion coefficients (*D*), hindering solute flow within the membrane. This phenomenon increases the solute resistivity (*K*) parameter of the membrane and promotes ICP ($K = \frac{\tau t_s}{\varepsilon D}$). They also have high viscosity at high concentrations which increases required pumping energy and reduces process efficiency. In further sections, different types of organic draw solutes are explained, and scientific work related to use of these solutes in CLPRO is reviewed.

a. *Simple organic ionic salts*

Islam et al. [23] explored organic ionic salts (Table 3) in closed-loop PRO and compared their performance with commonly used inorganic salts such as NaCl and NH_4HCO_3. They concluded that at concentrations that generate equal osmotic pressure (42 bars), these salts produce more water flux and power density compared to inorganic salts due to their lower RSF which was caused by the larger sizes of their hydrated ions. The salt fluxes of organic draw solutes were between 0.0325 $\text{mol m}^{-2}\ \text{h}^{-1}$ and 0.0854 $\text{mol m}^{-2}\ \text{h}^{-1}$ which are remarkably lower than NaCl (0.854 $\text{mol m}^{-2}\ \text{h}^{-1}$) and NH_4HCO_3 (0.952). Having a C-O double bond in their structures which makes the polarization of the anion better in their aqueous solutions, could be the reasonable explanation. Thus, more hydration of the solute's ions happens due the polarized nature. Also, it was observed that by increasing the draw solution concentration, the RSF remains almost constant for these solutes. In terms of water fluxes, obtained water fluxes for organic salts ranged between 19.02-25.09 LMH, while for NaCl and NH_4HCO_3, permeate fluxes were 17.50 and 16.40 LMH, respectively. Peak power density values (11.10-14.64 W/m^2) for these salts were 8.72% to 43.39% and 15.99% to 52.98% higher compared to NaCl (10.21 W/m^2) and NH_4HCO_3 (9.57 W/m^2) at 21 bars of applied pressure. Higher RSF for inorganic salts is the most critical factor causing the inferior performance of these salts. In conclusion, organic salts showed better performance regarding their minimal RSFs, higher water fluxes, and generated power densities

than their inorganic counterparts. In terms of power density, while considering thermal distillation as the regeneration process, authors concluded that NH_4C holds the highest potential for PRO application. However, the unavailability of membranes with enough mechanical strength, still remains a critical issue for harnessing the full potential of these draw solutes. At their solubility, these solutes produce osmotic pressures ranging from 70-1300 bars. Excluding calcium acetate (CaAc), the maximum generated power density can be achieved when the applied pressure is half of the transmembrane osmotic pressure difference. The most robust commercially available membrane can tolerate up to 48 bars [30]. Furthermore, this paper did not investigate the comparison of the performance of these draw solutes with inorganic ones at high concentrations such as 3 M. While at high concentrations, inorganic draw solutes result in higher salt flux. Organic solutions will have much more viscosity which increases required pumping energy and mass transport resistance. Thus, choosing the draw solute with better performance at high concentrations remains unresolved.

Switchable polarity solvents (SPS) are another category of simple organic draw solute. The SPSs can be separated from water through a reversible transition from water soluble to water insoluble by adding CO_2 [35-38]. The draw solute can dissolve into the miscible state using heat from low grade sources and N_2 gas to strip off the CO_2. Due to these properties, SPSs can be considered as great draw solutes in PRO.

b. *Hydro-acid complexes*

Hydro-acid complexes consist of metal(s) and ligand(s) parts that, when the metal center bonds to the ligand, the configuration of it expands. According to the required function, they can be manipulated by changing either metals or ligands. These compounds are highly soluble in water,

large enough to have negligible salt diffusion, easily regenerated, and provide a high osmotic pressure.

Han et al. [24] demonstrated a novel closed-loop PRO for sustainable osmotic energy production using $Na_5[Fe(C_6H_4O_7)_2]$ (Na-Fe-CA) hydro-acid complex as the draw solution. In all experiments, the TFC PRO hollow fiber membrane with a polyamide selective skin was used. In this study, the draw solute consists of a ferric complex with hydroxyl acids of citric acid (CA) as ligands. It was observed that this draw solute has a better performance compared to conventional inorganic draw solutes, such as NaCl, at the same molar concentration. Higher osmotic pressure of 58 bars at 1 M was achieved due to its hydrophilic groups with multi-charged anions, while for NaCl it is only 47 bars at the same concentration. The difference in osmotic pressure becomes even more at higher concentrations because CA ligands improve water solubility, generating higher water fluxes. At 1 M and 12 bars applied pressure, the obtained water flux was 48.6 LMH which is slightly more than NaCl (41 LMH). Based on the water flux and 12 bars applied pressure, produced power density was 16.2 W/m^2 and 13.7 W/m^2 for Na-Fe-CA and NaCl, respectively. Also, the hydro-acid showed negligible salt flux due to expanded octahedral structure. For NaCl, the RSF increased significantly with rising the applied pressure from 10.5 gMH at 0 bar to 32.7 gMH at 12 bars. On the contrary, Na-Fe-CA showed remarkably low salt diffusion ranging between 0.44 gMH at 0 bar to almost 3.0 gMH at 12 bars. Consequently, solute loss for the proposed system is minimal which reduces replenishment cost compared to conventional draw solutes like NaCl. The diluted draw solution was re-concentrated by adding ethanol for the precipitation of Na-Fe-CA. So, it can easily re-concentrated and it is not energy consuming. The regenerated draw solution used again in the process and in terms of J_w, J_s, and power density, the results were almost the same as the primary draw solution proving that the diluted raw solute was

recovered almost completely. On the other hand, Na-Fe-CA has a much larger molecular weight and a bulkier structure than NaCl. Therefore, at concentrations more than 1 M, for example 1.5 M, its viscosity is much higher (almost 5.5 times more) compared to NaCl, which increases the energy consumption in pumping and promotes ECP.

2.4.2.4 Functionalized nanoparticles

Recently, nanoparticles functionalized with hydrophilic groups have received significant attention, especially magnetic nanoparticles (MNP) due to their high surface-area-to-volume ratio and relatively easy separation from water by utilizing magnetic separation. MNPs are materials consisting of a magnetic core and a surrounding polymer shell. The magnetic separation can be achieved by using an external magnetic field due to the existence of nanoparticles in the magnetic core. The polymer shell not only decreases particle aggregation in the solution, but also enables surface modification for better osmotic performance. It seems that the particle agglomeration during the magnetic recovery remains the main problem in using MNPs, making the process economically not viable for long-term operation. Ling and Chung **[39]** investigated the use of ultrasonication and its effect on particle agglomeration. Although utilizing ultrasonication reduced nanoparticle agglomeration effectively, the magnetic properties were also decreased over time, limiting the total recovery by magnetic separation methods over several cycles.

2.5 Draw solution regeneration

In order to ensure sustainable production of electricity, diluted draw solutions must be re-concentrated periodically. The regeneration process has a crucial role in the energy efficiency of the whole system and the net energy generated in CLPRO systems. The recovery method must be energy efficient, cost-effective, and practical. It must not only re-concentrate the diluted draw solution completely (i.e. up to initial concentration of the draw solution), but also not allow salt

leakage while producing permeate water with high quality. If none of these conditions are satisfied during the regeneration, the effective driving force will decline, lowering the efficiency of the whole process. A summary of relevant regeneration processes for recovery of diluted draw solutions investigated in literature is shown in Table 4.

Table 4: Regeneration processes in the literature

Draw solutes	Regeneration process	Advantages	Drawbacks	Reference
NaCl	Thermal	Complete recovery of draw solution	Not energy efficient	[25]
$NH_3 - CO_2$	Distillation column		Not energy efficient and cost effective	[27]
KCit **CaAc** **KOxa** **KAc** **NH_4Ac** **NH_4C** **NH_4F** **KF** **NaGly** **NaP** **CaP**	MD MD MD MD Thermolytic Thermolytic Thermolytic MD MD MD MD	Independent of feed salinity, efficient rejection of non-volatile compound, use LGH	Low water flux, temperature polarization, membrane wetting	[23]
LiCl − methanol	MD	Minimal salt leakage	Very low efficiency, not economically practical	[26]
$CaCl_2$ **HCOONa** **KBr** **LiBr** **LiCl** **$MgCl_2$** **$Na(C_2H_5COO)$** **NaCl**	MD			[28]
NaCl **$MgCl_2$** **$MgSO_4$**	MD			[29]
NaCl	MD			[30]
NaCl	LGH	Low energy cost		[31]
$Na_5[Fe(C_6H_4O_7)_2]$	Precipitation	Effective separation, low energy consumption	Permeated water needs further separation	[24]

2.5.1 Thermal separation

Research has indicated that thermal separation could be good a choice for draw solution recovery [23,25,40,41]. During this process, heat can be utilized to turn volatile solutes into gaseous form, which can then be separated from the solution. Water evaporates through the distillation process, and for thermo-responsive polymers, draw solutes precipitate at a temperature

above the least critical solution temperature (LCST), allowing the separation via filtration to happen. Moreover, in switchable polarity solvents, heating removes the dissolved CO_2 which causes draw solutes to shrink and release water [42].

McGinnis and Elimelech [43] investigated FO as a method of seawater desalination process and its required energy compared with other desalination processes such as multi-stage flash (MSF), multi-effect distillation (MED), and RO. They simulated thermal recovery of the diluted ammonia-carbon dioxide draw solution using single vacuum column and multi-stage distillation (MSD) for very low temperature (40 ℃) and high temperature sources, respectively. In a low pressure single column system, the diluted draw solution is exposed to LGH counter-currently and volatile $NH_3 - CO_2$ mixture separates from water. Then, all gases were condensed under vacuum and removed with a steam thermojet. In multi-stage distillation the same configuration as MSF and MED is used. At the top stage a portion of feed water was vaporized by exposing to heat and then, the produced vapor was condensed in contact with second stage (lower temperature and pressure) on a heat transfer surface. This exposure to heat, vaporize more feed water, and so on. In MSF and MED unlike MSD, both energy and material streams move in series, while in MSD, partitioned parallel streams of the diluted solution enter each column. Potable water is produced out of 0.5 M NaCl as the simulated seawater, with the recovery rate of 75%, and concentration of less than 1 ppm. The FO draw solution inlet and outlet streams are 5 M and 1 M, respectively, at 25 ℃. For measuring the thermal desalination efficiency, a term of gained output ratio (GOR) was used which is defined as the ratio of each kg of steam condensed to each kg of water produced. Typically, the estimated GOR values for MSF and MED are between 8-15 at temperature of 70-120 ℃ [44], while the calculated range of GOR for FO is between 4.4-20.2 for temperatures between 40-250 ℃. They concluded that using low temperature (40-44 ℃) FO shows significant

energy saving. Compared to MSF, low temperature multi effect desalination (LT-MED), MED using thermal vapor compression (MED-TVC), and RO, the saved energy is 85.1%, 73.8%, 79.2%, and 72.1%, respectively. In addition, the electrical energy consumption for current desalination process lies between 1.6-3.02 kWh/m^3, while, for FO, due to benefiting from large recoveries and unpressurized fluid pumping, the electrical consumption is about 0.25 kWh/m^3.

McGinnis et al. [27] investigated the separation of $NH_3 - CO_2$ from diluted draw solution in PRO using distillation column. This draw solute can decompose at temperature and pressure of 60 ℃ and 1 atm, respectively, and be removed from water up to less than 1 ppm. Then, this water was circulated back to the feed side as the working fluid. In the modeling of OHE, some assumptions were made regarding the efficiencies of the pressure exchanger and turbine, 95% and 90%, respectively. The efficiency of the OHE calculated considering thermal and Carnot efficiencies. Thermal efficiency is the ratio of the amount of power produced by the engine over the heat used for recovering and separation draw solution and working fluid. Carnot efficiency is defined as the ratio of the engine over the Carnot engine which is the maximum theoretical efficiency. Thermal and Carnot (between 25 and 50 ℃) efficiencies of the OHE were calculated with the HYSIS® chemical simulator model and Aspen HYSIS®, respectively, considering a draw solution at concentrations ranged from 1 to 6 M (CO_2 basis). A distillation column, containing 30 theoretical stages, supplied heat at 50 ℃, bottom pressure and temperature of 10.62 kPa and 46.96 ℃, and top pressure and temperature of 10.54 kPa and 35.55 ℃ was considered as the recovery unit. When the effective driving force ($\Delta\pi - \Delta P$) approaches zero, the maximum engine efficiency is achieved which was almost 16% of Carnot engine (probable operation efficiency lies between 5-10%). With increasing the draw solution concentration, and consequently the increase of osmotic

pressure, water flux and power density will increase. However, using a more concentrated draw solution will increase the heat duty in the recovery unit as well.

It was concluded that the separation of NH_3 and CO_2 in the distillation column is inefficient. Some water vapor is also removed which consumes heat, and therefore, not all the supplied heat is converted to power generation. As the draw solution becomes more concentrated, the amount of vaporized water in distillation column also increases, and leads to the separation to the equivalent state, which lowers the efficiency of separation and results in decreasing the overall efficiency of OHE. On the other hand, higher draw solution concentrations will lead to higher power densities, requiring less membrane area and therefore, less membrane cost. Thus, a trade-off should be made between membrane capital cost and engine efficiency. Moreover, in thermal recovery, when using waste heat, one of the most important factors that should be considered is the efficiency of the heat exchanger, which affects its area and the capital cost of the system for suppling heat. The system efficiency has a direct relationship with the temperature difference between supply and rejecting reservoirs. The lower the difference, the lower the thermal efficiency of the heat engine is, which results in an increased heat exchanger area and cost [27].

MD is a thermal membrane process, in which water transfers across the membrane due to the vapor pressure difference across a hydrophobic membrane. The feed solution is in direct contact with one side of the membrane and draw solutes are prevented from penetrating inside the dry pores of the membrane, allowing vapor molecules to pass through it. The feed solution is prevented from flowing into its pores by a hydrophobic membrane due to the surface tension forces. Due to the many advantages of MD, some research groups utilize it as the method for re-concentration of the diluted draw solution. MD can reject non-volatile feed draw solutes up to 100% theoretically [45]. In addition, MD efficiency is independent of feed water salinity, allowing

the treatment of highly saline waters [45-47]. Membrane distillation also can use LGH, such as industrial waste heat, leading to a low energy requirement in the process [48,49]. However, this system has some drawbacks and limitations, such as: (1) low permeate flux compared to other separation techniques [50], (2) permeate flux decline due to temperature polarization, membrane fouling, scaling, and membrane wetting [50], (3) high heat loss by conduction, and (4) energy intensity because, although the pumping energy demand is similar to FO (0.25 kWh/m^3) [43], the energy required to heat the water from room temperature to 50 ℃ is 29 kWh/m^3. Many studies investigated OHE, trying to make it more feasible and practical using MD as the regeneration process for re-concentrating the diluted draw solution for PRO.

Hickenbottom et al. [51] performed a techno-economic analysis of OHE to recover low temperature waste heat. In this process MD is coupled with PRO to re-concentrate diluted draw solution utilizing LGH. They modeled an OHE system producing 2.5 MW of net power, the capacity of commercially available small-scale ORC (benchmark technology for this study) plants with twenty-year plant life, as the basis. In this modelling, 3 M NaCl was assumed as the working fluid in the PRO with operational pressure of 34 bars (~500 psi), and recovery rate of 15%. For MD, average water recovery of 6% based on the literature, and negligible membrane wetting were assumed. The temperature of feed and distillate streams were 70 and 30 ℃, respectively. LGH temperature (heat source) and cooling water system (heat sink) were assumed to be 80 and 20 ℃, respectively. Considering the base-case (2.5 MW of net power), the capital and O & M costs were estimated to be 57.3 and 3.6 million USD/yr, respectively. It was found that electricity is generated at the cost of 0.48 USD per kWh, which when compared with the average electricity cost for wholesale U.S. grid energy (0.04 USD per kWh [52]) or the organic Rankine cycle (ORC) (0.08-0.13 USD per kWh [53,54]), is not competitive.

The reason for high levelized cost of electricity is due to the energy required for pumping, which accounts for 40% of the gross electrical power produced. According to this study, the system efficiency is less than 1% due to low operating temperature. However, by increasing generated net power, PRO power density, and MD water recovery, the efficiency can be improved. Another study [55] demonstrated that the maximum theoretical efficiency is almost 9-10% when MD feed and distillate is 60 and 20 ℃, respectively, and 4 M NaCl is the working fluid in PRO. Operating with a draw solution, generating high osmotic pressure at high applied pressure, increases the PRO power density significantly and reduces membrane area, leading to better efficiency. Also, increasing the partial vapor difference across the membrane (i.e. operating at higher feed and lower distillate temperatures) will increase MD water flux and system efficiency and decrease the required membrane area. In another study, different draw solutes were tested in OHE, trying to assess better draw solutions for better system performance [28]. It was concluded that a lower RSF can reduce the MD load on the feed side, lowering the required pumping energy and membrane area. Therefore, the draw solutes with high RSF, such as inorganic ones, are not appropriate for solute recovery using MD, unless PRO membranes with higher selectivity were developed. According to the sensitivity analysis that was done on the operating parameters in this study, increasing PRO water recovery from 15% to 40% can decrease electricity cost by 20% (from 0.48 USD to 0.38 USD per kWh), and improve system efficiency by 32% (from 0.1% to 0.13%). Increasing MD water recovery from 6% to 30% has the same influence on electricity cost and system efficiency. In fact, electricity cost decreases 25% (from 0.48 USD to 0.36 USD per kWh), while efficiency will increase six-fold (0.1% to 0.6%). Increasing the operating pressure in PRO (up to 90 bars), significantly reduces electricity cost (0.48 USD to 0.21 USD per kWh), and triples system efficiency (0.1% to 0.3%). Although, increasing hydraulic pressure will increase RSF

resulting in higher feed stream bleeding and more heat duty in MD, the benefit of increased power density outweighs its drawbacks. Surprisingly, although increasing MD feed temperature leads to reduction in electricity cost, system efficiency (ratio of output work to input heat) would increase because, more heat is needed to increase the feed's temperature to the desired level.

Finally, this analysis shows that by increasing system size from 2.5 MW to 25 MW, 30% reduction in electricity cost would happen (from 0.48 USD to 0.34 USD per kWh). Considering the best-case scenario resulted from the sensitivity analysis, while, the system size, MD and PRO recovery rate, and operation pressure in PRO are 25 MW, 30% and 40%, and 76 bars, respectively, electricity generation costs would decrease remarkably from 0.48 USD to 0.1 USD per kWh (system efficiency increases from 0.1% to 0.8%). In conclusion, with currently available membranes and advancements, continuous operating OHE is not comparable with other technologies especially, ORC. Availability of highly permeable and selective PRO membranes with high mechanical strength can be promising in the viability of OHE. Also, draw solutions which produce higher osmotic pressure and possessing minimal RSF, play a crucial role in reducing PRO and MD membrane costs.

2.5.2 Physical separation: Reverse osmosis

Several studies investigated the PRO-RO hybrid system [56-60]. The energy consumption of conventional SWRO using one pressure exchanger (PX) is 2.5 kWh/m^3, while the thermodynamic minimum specific energy consumption (SEC) for this system under 50% recovery is ~1.1 kWh/m^3[61]. This amount is higher than the energy produced by PRO. In fact, according to a previous study [56], closed-loop PRO can address only 50% of the SEC required in RO for seawater desalination when the water recovery is 50%. Furthermore, because of the membrane sensitivity and severe fouling, highly saline draw solutions cannot be used in this system. On the

other hand, the hybrid RO-PRO system can be used for recovering required energy in RO via utilizing energy recovery device (ERD), as well as dilute the RO brine to sea water concentration to allow its discharge back to sea.

Wang et al. [57] investigated integration of RO-PRO system with double ERDs regarding specific energy reduction using temperature enhanced PRO. The concentration of feed and draw solutions are 0.01 M NaCl (municipal wastewater) and 1.2 M NaCl (RO brine), respectively. There are some parameters that affect the hybrid system SEC such as PRO permeate and operating pressure and temperature. The amount of PRO permeate has a direct relationship with power density and hence, with the whole system SEC. It is stated that in a situation that PRO and RO permeates are equal along with 50% recovery 30 bars of applied pressure in the PRO unit, the lowest SEC of RO-PRO system can reach 1.57 kWh/m^3. This amount deviates from the theoretical limit of SEC (1.14-1.20 kWh/m^3) mentioned in the literature [58,59], which is due to the SWRO capacity or low RO permeate flow (RO recovery assumed to be 50%). By increasing the capacity from 1500 to 150,000 m^3/d, SEC decreases 1.27 kWh/m^3. Likewise, increasing operating pressure from 30 to 35 bars leads to SEC reduction by 12.94% (from 1.27 to 1.11 kWh/m^3), resulting from the higher generated power density. However, increasing the operational pressure will decrease the permeate flow significantly. On the other hand, higher temperature leads to higher water permeate due to improved membrane selectivity and transmembrane effective osmotic pressure. It was stated that when using 1.2 M NaCl (RO brine), increasing temperature from 25 to 50 ℃ while increasing applied pressure from 28.5 to 29 bars, the permeate flow will rise from 501.8 to 878.4 m^3/d and consequently, leads to power density increase (from 16.55 to 29.84 W/m^2). This result implies that elevating temperature along with moderate pressure can improve water permeability

and power density significantly. In terms of SEC, increasing temperature to 50 ℃ will result in SEC reduction by 17.93%.

Renewable energy sources such as wind and solar can be coupled with RO to compensate electricity demand in this system [62-65]. However, these sources are not always available (solar power at nights). Thus, another source of renewable energy should be integrated with this system. Some studies investigated PRO-RO hybrid system coupled with solar PV [66,67]. Tong et al. [67] proposed a PRO-RO hybrid system coupled with solar PV in a large-scale plant with a capacity of 5000 m^3/d . In this system, solar energy is used to heat up the inlet streams in PRO to improve its performance by increasing the osmotic pressure. Tertiary wastewater (0.02 M) and seawater (0.61 M) are the feed and draw solutions in this system. In order to calculate the maximum amount of recoverable energy, PRO membrane or module inefficiencies were neglected. According to the presented results, when the PRO operating temperature (T_H) increases from 293.15 K to 353.15 K, the maximum generated energy (when the applied pressure is half of the osmotic pressure difference) increases from 0.183 to 0.221 kWh/m^3 because a higher temperature leads to higher osmotic pressure which results in a higher power density. Increasing the operational pressure and RO recovery rate will increase the net SEC of the system, while elevating the temperature has the opposite effect. For instance, increasing temperature from 293.15 K to 353.15 K, considering the optimal value of applied pressure at each temperature, and when the recovery rate is 0.5, the net SEC reduces from 0.47 kWh/m^3 to 0.39 kWh/m^3. However, increasing temperature will reduce the second law efficiency (η); For the same range reduction in temperature, η will decrease from 9.16% to 3.14%. This can be justified by the fact that increasing T_H, decreases the implementation efficiency of the solar thermal energy due to more required heat duty to maintain the elevated temperature. Consequently, solar collectors with a larger area are needed which increases the one-

time infrastructure cost. Therefore, an optimization between net SEC and η should be made while choosing the operation temperature. The analytic hierarchy process (AHP) was made to choose the optimal T_H, considering net SEC, η and the area of the solar collector. It was concluded that higher T_H is beneficial to the system. Another system is also considered using the hybrid system, taking seawater as the RO feed and utilizing RO brine and treated wastewater as the draw and feed solutions while getting heated by solar energy prior to PRO. The achievable net SEC for this system, when T_H and RO recovery are 353.15 K and 50%, respectively, is 1.34 kWh/m^3 which is higher than the previous hybrid system (0.39 kWh/m^3). The reason behind this result is that the dilution effect in PRO was neglected. Although more energy could be generated in PRO due to higher osmotic pressure difference, higher energy consumption in RO makes the overall SEC more.

2.5.3 Chemical separation: Precipitation

Precipitation is one of the most energy-efficient methods for recovery of draw solutes. The draw agents precipitate by adding another compound, changing the solution pH or temperature, which allows water to be separated from draw solutes. Han et al. [24] utilized precipitation for the regeneration of a Na-Fe-CA hydro-acid complex. By adding ethanol to the solution of $Na_5[Fe(C_6H_4O_7)_2]$, draw solutes start to precipitate because they cannot dissolve in ethanol. The re-concentration process worked effectively (yield>99%) without requiring an energy input. However, a small amount of water/ethanol in the mixture can be lost due to evaporation. In other studies [68,69], the precipitation and regeneration of $MgSO_4$ and $CuSO_4$ were investigated by adding $Ba(OH)_2$. After the draw solutes precipitated, the soluble $Ba(OH)_2$ in water will precipitate through the addition of CO_2. This regeneration process suffers from some disadvantages, such as the product water contains residues of heavy metal ions. Moreover, the removal of $Ba(OH)_2$

cannot be completely achieved and a portion of it remained soluble. Thus, the recovered water still needs further purification [70]. In addition, a large amount of $Ba(OH)_2$ is consumed because of metathesis precipitation. Although this method is energy-efficient, this process suffers from low water recovery and the precipitate costs may be very high. Moreover, in most cases, a downstream process is needed to separate draw solutes completely from produced water.

2.5.4 Magnetic recovery

Magnetic nanoparticles (MNPs) can be functionalized with hydrophilic species to create superparamagnetic nanoparticles to enable easy recovery by an external magnetic field in magnetic separators. In the matter of energy consumption, this method is effective. However, it has some drawbacks. The most important problem is particle agglomeration which reduces driving force drastically after a couple of cycles. In this process the separation efficiency can be low regarding the separation of the smaller particles because the magnetic force was not dominant among diffusion force and gravity. Therefore, the product water may need to be further processed [71].

2.6 Energy consumption of the regeneration process

The viability of CLPRO is strongly dependent on the energy consumption of the regeneration processes used to recycle the draw and the feed solutions back into the system. In fact, this dependency manifests in the fact that the overall energy produced should compete with other renewable energy sources. As presented in the previous section, many regeneration processes have been used in CLPRO. Several authors have not discussed the impact of the energy consumption of the used regeneration processes on the overall produced energy. Herein, the feasibility of some potential regeneration processes based on the net energy production is discussed. For that, first, the maximum theoretical energy production is identified as the upper value of energy that can be produced by PRO under perfect conditions such as ideal membrane,

ideal salt rejection, and perfect hydrodynamics. This energy can be expressed as a function of the osmotic pressure difference between the feed and draw solutions as follows [71]:

$$SE_{PRO}^{M} = \frac{1}{4}\left(\frac{(\pi_D - \pi_F)^2}{\pi_D + \pi_F}\right) \quad (1)$$

where π_D and π_F are the draw and feed osmotic pressures, respectively. In real conditions, this maximum is unachievable due to fouling, scaling, salt diffusion, and imperfect hydrodynamics. For that, it is assumed that optimized PRO systems can produce 70% - 80% of the maximum extractable energy [17]. Then, the first condition to discuss the feasibility of CLPRO is to satisfy the following criterion:

$$SE_{PRO}^{R} - SEC_{RP} > 0 \quad (2)$$

SE_{PRO}^{R} and SEC_{RP} are the PRO specific energy production and the specific energy consumption of the regeneration process, respectively. Figure 4 shows the energy consumptions of various regeneration processes used in the literature, as well as the PRO specific energy that can be theoretically and practically produced with potential draw solutions. To satisfy Equation 2, thermal processes and reverse osmosis are excluded. In fact, the SEC of RO process ranges between 2.4 and 3.4 kWh/m^3, which makes the net power production negative, thereby deeming the process energetically inefficient. Similarly, thermal processes such as MD or MED have a very high energy consumption (100 to 1000 times the energy produced by PRO), which is unsuitable for a viable CLPRO.

Several studies suggested that MD can operate with low grade waste heat released from industrial activities (i.e., nuclear plant, thermal power plant factories, etc.) and therefore can be used as a downstream separator for PRO. This seems too ambitious due to two reasons: 1) MD

should be fully powered by waste heat, which is not practically achievable, and 2) if we assume that the previous condition is fulfilled, that waste heat should be unrecoverable by any other process because if so, around 100 kWh/m^3 of recoverable energy will be consumed to produce less than 2 kWh/m^3. For that, MD is likely unsuitable for PRO. Similarly, besides the high energy consumption, the range of RO applicability is limited (<100 bars). Also, like MD, the use of renewables is not reasonable. For the other possible regeneration processes like precipitation, waste heat to degrade thermolytic solution, and electromagnetic regeneration, the energy consumption is relatively attractive (< 0.2/0.4 kWh/m^3). However, these processes are still suffering from low recovery rate as well as various practical drawbacks (agglomeration, cost efficiency, low recovery ratio, etc.). Figure 4A shows two main zones: the zone of inefficiency and the targeted zone. The zone of inefficiency is where the SEC of a system used for solution recovery does not satisfy criterion 1 as mentioned in Equation 2, and the targeted zone is characterized by the regeneration process handling solutions with high osmotic pressure with low energy requirements.

The second criterion that should be considered is the economic competitiveness of CLPRO. More precisely, the cost of the produced energy must be comparable to the renewable energies, such as wind, solar, and hydroelectricity. As a comparison tool, economists use the levelized cost of electricity (LCOE) to compare between energy harvesting processes. To determine the LCOE, an estimation of the cost is required. Several studies have performed a techno-economic evaluation of PRO process [51,71-74]. The analysis showed promising results with high solutions with osmotic pressure ($\Delta\pi$ > 150 bars) [73]. However, these studies have considered OLPRO and very few studies have been performed for CLPRO [51,74]. As shown in Table 2, CLPRO has some economic advantages when compared to OLPRO such as lower capital and operation costs, as well

as a controllable produced energy (by controlling the input osmotic pressure). Therefore, the choice of the draw solution and the way to regenerate it is a determining factor for the cost effectiveness of CLPRO. Overall, higher osmotic pressure with a low SEC of regeneration is the key for a sustainable, viable, and competitive renewable source of energy. The van't Hoff relationship was used to calculate the osmotic pressure. For a highly concentrated solution, there is a gap between the real osmotic pressure and that provided by the van't Hoff relationship. Therefore, the energy produced must be greater than the energy calculated using Equation (1). Future studies should be performed to quantify the real extractable energy at high draw solution concentrations.

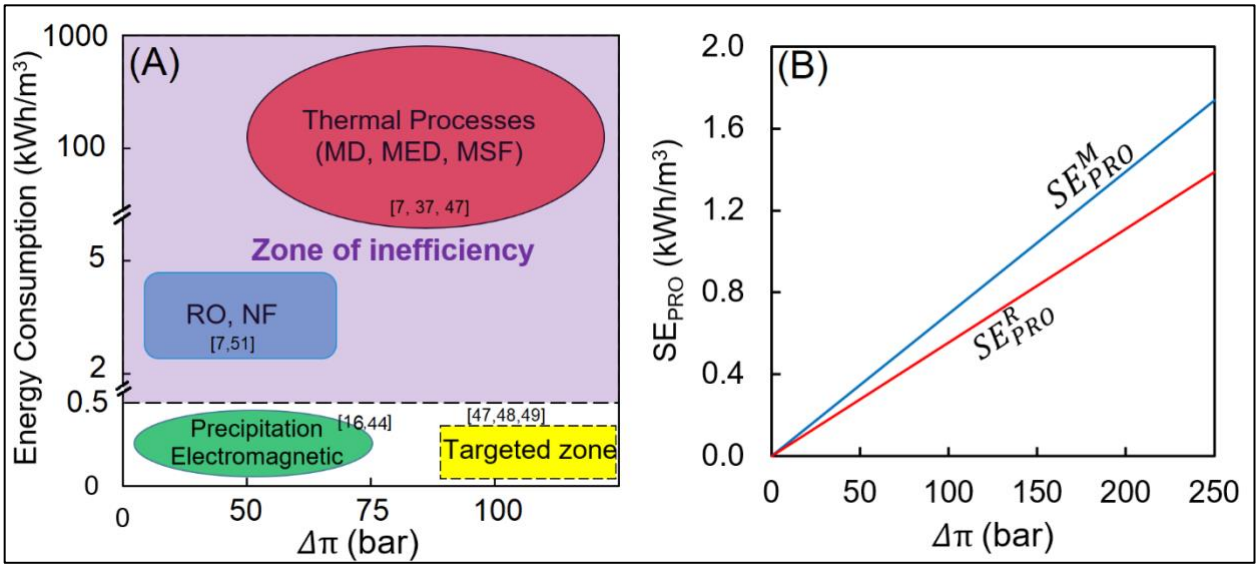

Figure 4: Specific energy consumption of draw solution regeneration processes, SEC, and the specific energy production of PRO, SE_{PRO}. (A) The SEC of potential recovery processes used in the literature. (B) Shows the maximum and the real achievable energy by PRO. Here the real energy is considered 80% of the maximum theoretical extractable energy as shown in previous work [17]. The calculation that the PRO feed solution is pure water is assumed. The van't Hoff relationship was used to calculate the osmotic pressure for 25°C.

For the specific case of an OHE, presented in Figure 5A, where the PRO is coupled to MD to generate electricity from LGH, the thermal efficiency, η_{OHE}, is defined as the ratio between the

generated power through PRO- turbine and the heat duty for separating and recycling the diluted draw solution via MD:

$$\eta_{OHE} = P/q_h = Y\pi/c_p(T_H - T_C)\,\rho_W \quad (3)$$

Here, P, q_h, Y, π, c_p, ρ, T_H, and T_C are respectively the power produced by the PRO-TB component, the amount of heat, the mass flow recovery of MD, the osmotic pressure of the working fluid (water in this case), the heat capacity of the working fluid, the working fluid density, the heat source temperature, and the cold sink temperature. Carnot efficiency is the relative comparison of an engine efficiency with maximum theoretical efficiency of the Carnot engine which operates with the same high and low temperatures heat streams ($\eta_{Carnot} = 1 - T_C/T_H$). Carnot efficiency is presented as a reference. For comparison, the energy conversion efficiency of Organic Rankine Cycle (ORC), operating in the same range of temperature was plotted. This efficiency was determined from the Entropy-temperature diagram for and ideal ORC process operating with isopentane as a working fluid. The Carnot efficiency has little practical value due to the fact that, even being very efficient, a Carnot engine has to operate at infinitesimally low velocities to allow the heat transfer to occur, then, no power will be generated (i.e., a thermodynamically reversible process). For that, the Carnot efficiency at maximum power output of Carnot engine (dashed red line) is defined as:

$$\eta_{Carnot}^{Pmax} = 1 - T_C/T_H \quad (4)$$

This efficiency is more practical than the classic Carnot efficiency since it describes the performance of the engine when power is produced. Figure 5B shows, as for any heat engine, the increase of the temperature difference leads to the increase of the OHE efficiency. This efficiency is still remarkably lower than η_{Carnot} due to losses occurring during the processes (heat losses: in MD, heat exchanger, hydraulic losses: in PRO due to constant applied pressure that leads to friction

losses, unutilized energy, pressures losses in the PRO module). However, the OHE efficiency is still greater than η_{Carnot}^{Pmax}, which means that the OHE reaches higher efficiency for PRO energy production lower than its maximum. Therefore, pushing PRO for maximum energy production should not be the target for an OHE. However, tracking the optimal PRO energy generation for maximum efficiency is one of the important operational parameters that should be readily controlled. Consequently, the required applied pressure in the PRO side for maximum efficiency is lower than the half of osmotic pressure difference between the draw and the feed side, a condition widely utilized for PRO energy optimization.

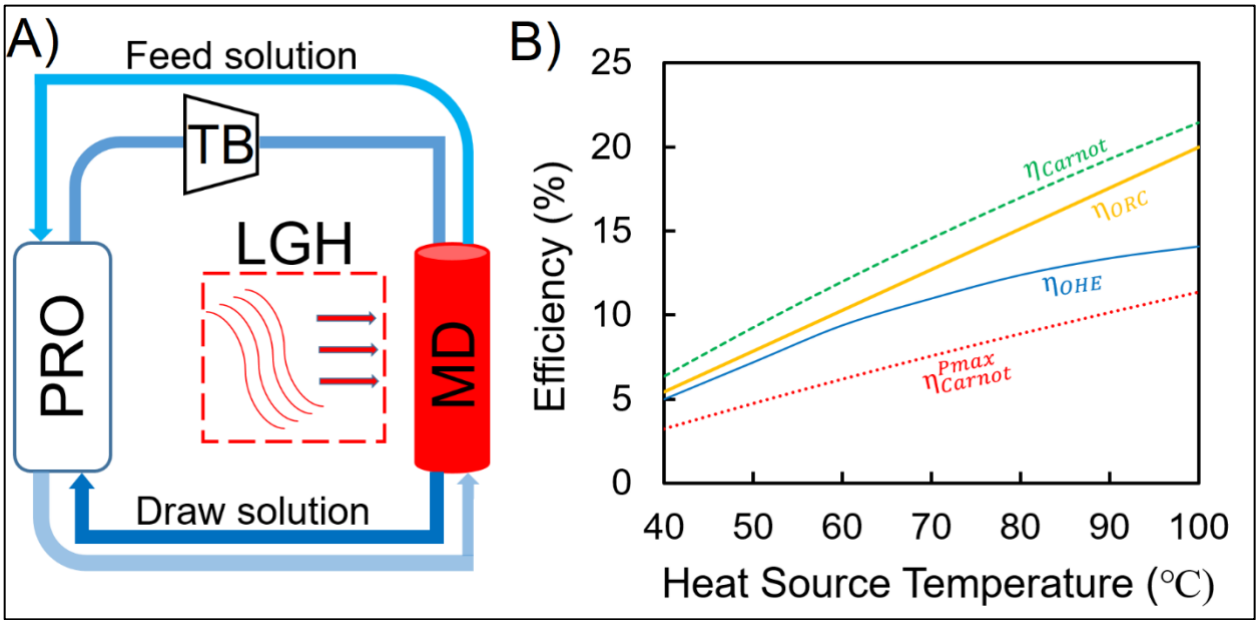

Figure 5: (A) Schematic of a MD-PRO OHE. (B) Energy efficiency of the PRO-MD OHE at different heat source temperatures of the working solution (4M NaCl, osmotic pressure π = 200 bar), Carnot efficiency of the OHE, and the Carnot efficiency at maximum power produced. Also, the energy conversion efficiency of ideal Organic Rankine Cycle with isopentane as a working fluid. The temperature of the cold sink is 20 °C. The mass recovery rate of MD process and the thermodynamic properties of the process were adopted from [30]. The relative flow rate (the ratio between the permeate mas flow and the feed mass flow) was assumed to be 0.918.

The comparison between OHE and ORC in the same temperature range shows the main zones: below and beyond 70°C. In the first zone, OHE efficiency is slightly lower than that of ORC (1-3% of efficiency difference) which means that of OHE can be practical alternative for ORC to harvest energy from low temperatures specially when considering that ORC is unable to

tolerate fluctuations in the heat source temperatures, the operational constraints imposed by the working fluids, as well as the economic unviability of ORC for low temperatures [75]. In the second zone, it is clearly seen that ORC has a much better efficiency than OHE that makes it incapable of competing with binary cycle processes at relatively high temperatures. Note that the previous statements are valid for OHE operating with water as the working fluid characterized by an elevated heat of vaporization which causes losses in the membrane side as well as in the heat recovery device (heat exchanger). For that, losses may be mitigated by employing other working fluids with a low heat of vaporization. However, this working fluid should also provide high osmotic pressure to optimize the energy production in the PRO side as well as guarantee a certain tolerance to MD membrane (fouling and wetting). Undoubtedly, developing a PRO membrane withstanding high pressures is a vital condition toward the viability and the competitiveness of OHE. Overall, CLPRO, including the specific case of OHE, seems to have great potential to produce energy from salinity gradients as well as harvesting power from heat waste and has the potential to compete with other sources of renewable energy and energy conversion processes. This also is still relying on the economic viability of CLPRO and OHE that is not definitely proven.

2.7 Wastewater as the Feed Solution in Pressure Retarded Osmosis

Some studies implemented treated wastewater as the feed solution in PRO [17,21,94]. Matsuyama et al. [91] used seawater as the draw and sewage-treated water as the feed solutions to evaluate hollow fiber membrane performance and calculate net output power. They carried out the tests with applied pressure of 15, 12.5, and 10 bars at the temperature of 25 ℃. The membranes effective are 600 m^2. They reported that at 15 bars of applied pressure, the power density and net output power were 3.1 W/m^2 and 0.07 W/m^2. They also proposed a target value for power density. According to their calculations, the net output power could be 2.8 W/m^2, if the achieved

power density be 6.5 W/m^2. With this net output power for systems using 300,000 m^3 and 1,000,000 m^3 of seawater per day, the power generation cost based on Loeb model would be 0.25 and 0.20 $/kWh. The target values were calculated based on water permeability coefficient (A) and salt permeability coefficient of the membrane which are 5 and 0.25 times the current values of the membrane ($A = 2.05 \times 10^{-6}\ {}^{m}/_{s.\,Mpa}$, $B = 5.5 \times 10^{-9}$ m/s). They concluded that with these A and B, the net output power can reach 2.8 W/m^2 and the proposed system can be scaled-up.

Sakai et al. [92] investigated the utilization of Fukuoka SWRO brine plant instead of seawater as the draw solution. The proposed system was for two reasons: (i) SWRO brine produce more osmotic pressure that seawater and consequently more water flux and power density can be achieved and (ii) the SWRO needs to be diluted to seawater concentration prior to discharge not polluting sea. Using a 10-in module, they achieved the maximum power density of 13.5 W/m^2 with the applied pressure of 25 bars. According to their experimental data, the net output power in PRO (the difference between generated power and required energy for pumping) when the power density is 10.1 W/m^2 was higher than the best case scenario (13.5 W/m^2) due to optimized values of permeation ration (~ 0.67) and concentrated brine flow rate (40 L/min per module). The calculated generation cost for power density of 10 W/m^2 and 30,000 m^3/d of concentrated brine was 0.25 $/kWh. It was predicted that with a modified membrane, power density of 12 W/m^2 is achievable. Considering 1,000,000 m^3/d of concentrated brine from SWRO, electricity generation cost could be 0.088 $/kWh. In another study [93], the integration of SWRO with PRO to reduce the energy consumption of desalination plant was investigated in Japan over a year based on proposed system from previous study [92]. RO brine and treated sewage water were proposed as the draw and feed solutions, respectively. It is concluded that the integration of PRO to SWRO

can lead to a 10% reduction in desalination energy consumption. They concluded that by using 1,000,000 m^3/d of concentrated brine, if the cost of membrane is reduced to 550 $/module, the generation cost can be 0.09 $/kWh which is reported by a previous study [92]. Currently, the Mega-Ton plant with the membrane cost of 3200 $/kWh and same daily brine flow rate, generates electricity at the price of 0.19 $/kWh (for both cases the power density is 12 W/m^2).

Wan and Chung [21] experimented with a PRO system comprising of seawater brine (SWBr) and wastewater retentate (WWRe) as the draw and feed solutions, respectively, by carrying out the PRO test using different solutions at 20 bars applied pressure and calculating power density. First, 1 M NaCl and DI water were used as the baseline and the achieved power density was 27 W/m^2. Then, they replaced NaCl solution with SWBr and 0.81 M NaCl (equivalent to SWBr salinity) and the generated power densities were 21.3 W/m^2 and 21.1 W/m^2, respectively. In these trials water flux decreased from 64 LMH to 40 LMH due to salinity reduction in the draw solution. In the next two tests they replaced the DI water with WWRe. In this condition, water flux dropped drastically by 75-80% due to the fouling in the membrane support layer. The maximum achievable power density was 4.55 W/m^2. Therefore, they decided to pretreat the WWRe with UF and NF and do the PRO test again with 0.81 M NaCl as the draw solution. The achieved power density after the NF treatment was 9.31 W/m^2. After that, they replaced the simulated RO brine (0.81 M NaCl) with the actual SWBr. In this condition, PRO generated 8.9 W/m^2 of power density. The slightly reduced power density was due to metal cations in the SWBr which can react with the organic foulants in the feed solution and enhance the fouling.

Chapter 3: Methodology

3.1 Materials

The mining wastewater was provided by Agnico Eagle Mines Limited (Rouyn-Noranda, QC, CA). The samples were from the wastewater treatment system after the cyanide removal process. There are three kinds of commercialized membranes were used in the experiments. The UF membrane was provided by Synder Filtration Inc. (Vacaville, CA, USA), for nanofiltration process, TFC membrane (NF90) from Dow Filmtc™ (Minneapolis, MN, USA) was used, and in the PRO experiment, highly permeable FO membrane and spacer sheets were purchased to be utilized in the PRO tests. The membrane specifications are illustrated in the Table 5. For synthesizing the draw solution, ammonium carbonate ($(NH_4)_2CO_3$) and was purchased from Fisher Scientific Co. (Toronto, ON, CA). DI water (Millipore, Billerica, MA) was utilized in the draw solution preparation. A calibrated conductivity meter (Oakton, Eutech Instruments) was used to measure conductivity.

Table 5: Membrane specifications

Manufacturer	Synder Filtration	Dow Filmtc™	FO Membrane
Salt Rejection (NaCl)	-	97%	99.6 ± 0.15%
Structural Parameter (S)	-	-	215 ± 30 microns
Maximum Operational Pressure	120 psi	600 psi	180 psi
pH Operating Range (Ambient Temperature)	2-10	3-10	2- 11
Maximum Operational Temperature	55 ℃	45 ℃	70 ℃
Pore Size/Molecular Weight Cut-off	20 kDa	~200-400 Da	-
Polymer	Polyethersulfone (PES)	Polyamide (PA)	-

3.2 Feed and Draw Solution Preparation

Prior to the UF process, the received wastewater effluent from the mine was filtered using a polyamide microfilter (Sartorius, Oakville, ON, CA) with a pore size of 0.45 μm via a vacuum filter. In this step, large suspended solids which will cause membrane clogging in the further steps were separated from wastewater. This filtration is necessary and prevents irreversible fouling on the UF membrane [101]. Then, the filtered solution was used as the feed in the UF process to separate particulates, colloids, bacteria, proteins and polysaccharides. Next, the UF permeate was used as the feed solution in NF process. In this stage, sugars, amino acids and Monovalent, divalent, and multivalent ions were separated from the solution. Also, heavy metals were targeted to be separated in this step. These stages are the pre-treatment steps to prepare the feed solution (NF permeate) for the PRO step. The process schematic is illustrated in Figure 6. Three liters of draw solution with a concentration of 3M were prepared by mixing 9 moles (864 g) of $(NH_4)_2CO_3$ powder with DI water in a beaker. Then, the solution was mixed via a magnet on a magnetic stirrer overnight. Each test was repeated three times.

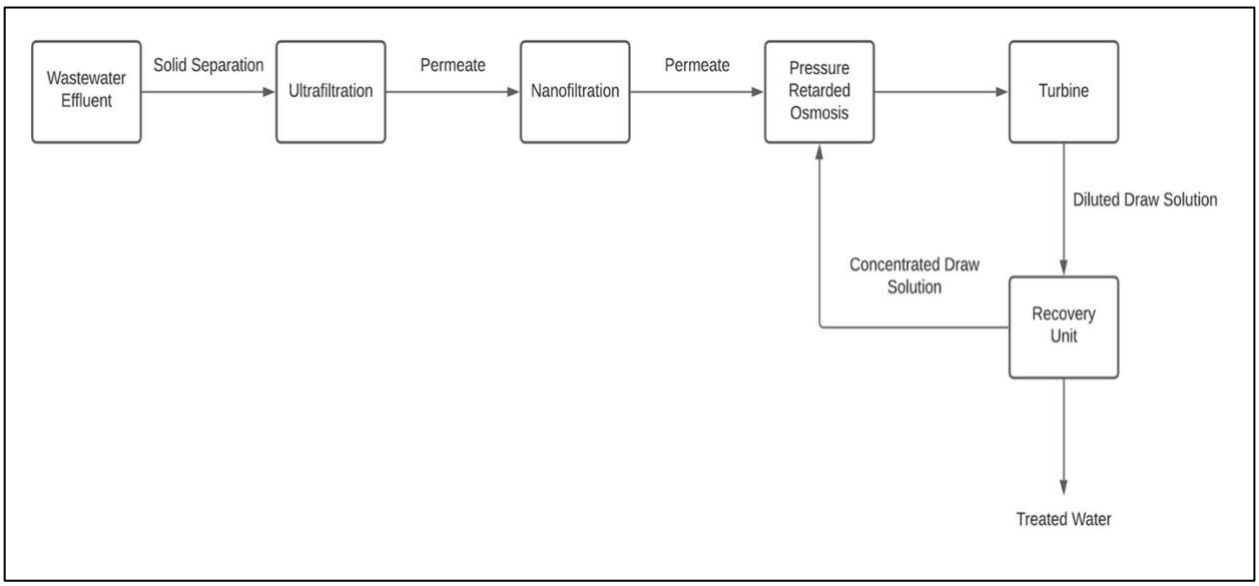

Figure 6: Schematic of the whole process

3.3 IC and ICP-MS analyses

By using ion chromatography (IC) and inductively coupled plasma mass spectrometry (ICP-MS) analyses, ions and heavy metals in the water were identified, respectively. For each analysis 10 mL of samples were collected. In ICP-MS analysis, the samples are introduced to high temperature, argon-based plasma through pneumatic nebulization. The target elements dissolves and ionized due energy transference from the plasma to the sample stream. Using mass spectrometer (quadrupole or magnetic), the resulting ions are separated from plasma based on their mass-to-charge ratio. The separated ions are counted by an electron multiplier detector. The resulting information is processed by computer. For this analysis, samples from untreated wastewater, UF permeate and NF permeate were collected and diluted by the factor of 2, meaning 1 mL of sample was mixed with 1 mL of DI water.

Ion chromatograph (IC) is a form of liquid chromatography which measures the concentration of ions based on their interaction with resin (stationary phase) and the eluent (mobile phase). There are anion column and cation column (each time only one of them) which attracts anions and cations, respectively. Depending on their affinity for the specific resin, ion moves in the chromatographer column with different speeds and they will be separated based on their size and ion charge. Then, the eluent passes through the column and ions with weaker affinity to the column, eluted faster and vice versa. A conductivity detector will measure the ions as they exit the column and plots conductivity vs. time. Each ion produces a peak on the graph, showing its concentration in the injected solution. In the tests, oxalic acid and sodium carbonate were the eluents for determining cations and anions, respectively. Samples from the untreated wastewater, UF permeate and retentate, and NF permeate and retentate were taken after each 6-hour run and diluted by the factor of 20, meaning 0.5 mL of sample was mixed with 9.5 mL of DI water. For

both tests, dilution is necessary for the detectors due to their measurement limits. After the data was collected, each value was multiplied by the dilution factor to obtain the actual concentrations.

3.4 Ultrafiltration and Nanofiltration Experiments

A bench-scale RO setup was used to carry out both UF and NF experiments. The schematic of these processes is illustrated in Figure 7. The UF and NF membranes were soaked in DI water for 20 minutes and after that, placed in the cross-flow cell with the effective membrane area of 33 cm^2. For the UF test, 5 liters of wastewater were poured into the feed container which was connected to the high-pressure pump (Hydra-cell, Toronto, ON, CA). In NF, 4 liters of UF permeate was used as the feed. Wastewater and UF permeate were pumped to the cell at pressures of 120 psi and 300 psi for UF and NF tests, respectively. A pressure gauge was placed after the cell to monitor the applied pressure on the membrane. After the pressure gauge, a flow meter was used to maintain the flow at the rate of 1.0 $L/(m^2.h)$ (LMH). A chiller (Cole-Parmer Instrument Company, Vernon Hills, IL, USA) was used to keep the temperature constant at 20 ℃. After the chiller, the solution flows into the initial container and ends the cycle. The permeate exited from top of the cell and was collected in another container which was placed on a balance (Sartorius, Oakville, ON, CA). The balance was connected to a laptop via USB port and data was recorded in Microsoft Excel every 1 minute for the duration of 6 hours. Data collection started once the pressure increased to the desirable amount and system became stable after all the bubbles were removed. The operation time could not exceed 6 hours because, after 6 hours, the chiller could not maintain the temperature at the set amount and fluctuated severely. Thus, the results were not valid. Using the equation 6, the permeate fluxes over 6 hours were calculated:

$$J_w = \frac{\Delta m}{\rho A_m \Delta t} \tag{6}$$

Where J is the water flux, Δm is the amount of permeate in each interval, ρ is the density, A_m is the membrane effective area, and Δt is the data collecting intervals which is 1 min. The water recoveries for both UF and NF over a 6-hour period were calculated using the following equation:

$$\text{Recovery } \% = \frac{\Delta V}{V_1} \tag{7}$$

where ΔV is the total permeate after 6 hours and V_1 is the initial feed volume. A mass transfer balance calculation was done to estimate the amount of each solute scaled on the UF membrane surface. In order to that, concentration of each solution (retentate, permeate and initial wastewater) was multiplied by its volume to calculate the mass of each ion. Subtracting the masses in the retentate and permeate from the initial wastewater will give the amount on the membrane.

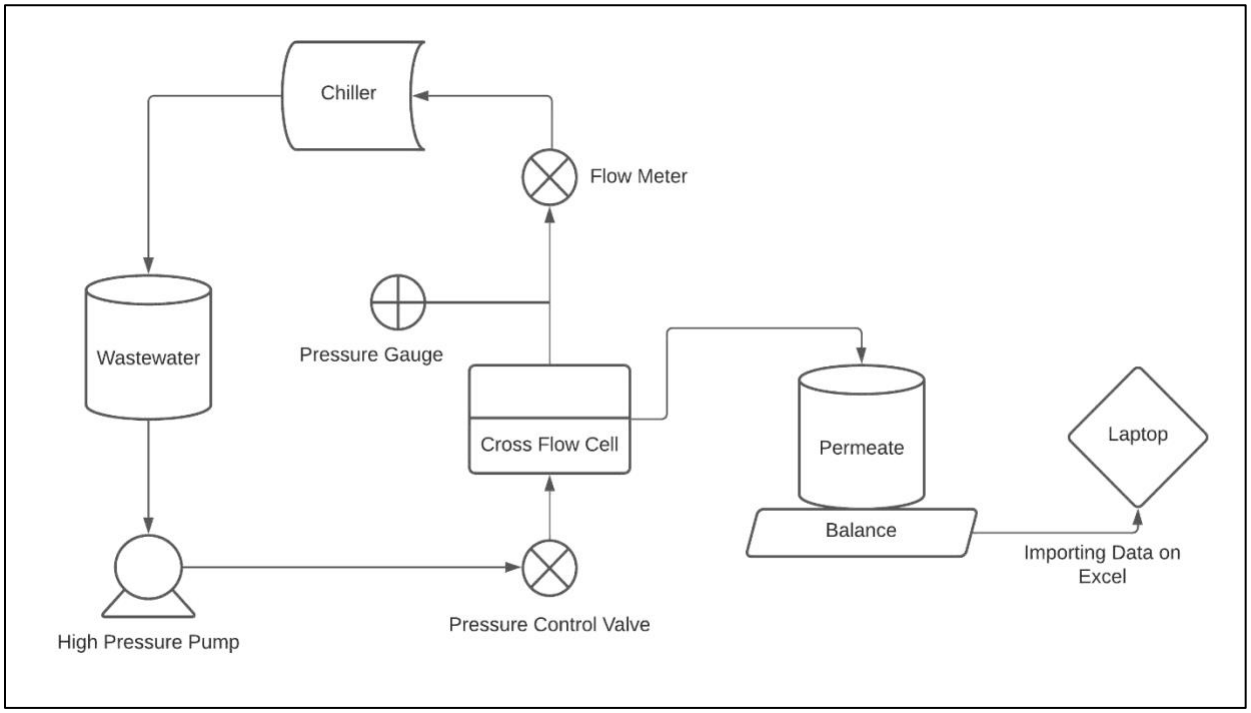

Figure 7: The schematic of UF and NF tests

3.5 PRO Experiment

The schematic of the PRO experiment is shown in Figure 8. First, the membrane was soaked in DI water for 20 minutes as suggested from the manufacturer to achieve its best performance. Then, the membrane was rinsed with DI water prior to placement in a cross-flow cell with an effective surface of 33 cm^2. The active layer of the membrane is facing the draw side and the support layer facing the feed side. Spacers provided by Porifera are placed below the membrane in the streams channels to avoid the membrane from direct contact with streams. A meshed metal sheet is placed above the membrane to keep the membrane steady while applying pressure on it, avoiding membrane rupture. A variable speed gear pump (Cole-Parmer Instrument Company) is used for circulating the feed solution in a closed-loop cycle at the rate of 1.0 LMH. The draw solution on the other hand, is circulated and pressurized by the high-pressure pump at the constant pressure of 180 psi, and the flow is maintained at 0.8 LMH. A chiller is used to maintain the draw solution temperature at 20 ℃ to omit temperature's effect on the experiments and also, prevents HP pump from heating up. At the beginning of the test, 3 liters of NF permeate as the feed solution and synthesized draw solution wee poured into the containers. The pressure was increased gradually up to 180 psi using the valve placed on the pump. Once the system became stable, the trans-membrane water flux is measured over 6 hours with a balance and calculated using equation 6. The water recovery is calculated using equation 7. The amount of generated power per unit of membrane area (W/m^2) can be calculated by multiplying the water flux by the applied pressure [76]:

$$W = J_w \times \Delta P \tag{8}$$

In order to evaluate the fouling effect of the wastewater on the FO membrane support layer and consequently, the PRO performance, and to calculate RSF of the draw solution, the PRO test was

carried out with DI water as the feed solution with the same conditions. The water flux and power density were calculated in the same way as the previous test. At the end of the test, the feed solution conductivity was measured using the conductivity meter. Using the following equation, the RSF was calculated:

$$J_s = \frac{C_f V_f - C_{f.i} V_{f.i}}{A_m \Delta t} \quad (9)$$

Where C_f and V_f are the concentration and volume of the feed at the end of the test (6 hours), respectively, $C_{f.i}$ and $V_{f.i}$ are the initial concentration and volume of the feed, respectively. Conductivity and concentration have a linear relationship. Thus, the conductivity of two solutions with known concentrations (0.5M and 0.01M) was determined using the conductivity meter, and the line equation was defined. Then, the conductivity of the feed at the end of the test was measured to calculate C_f.

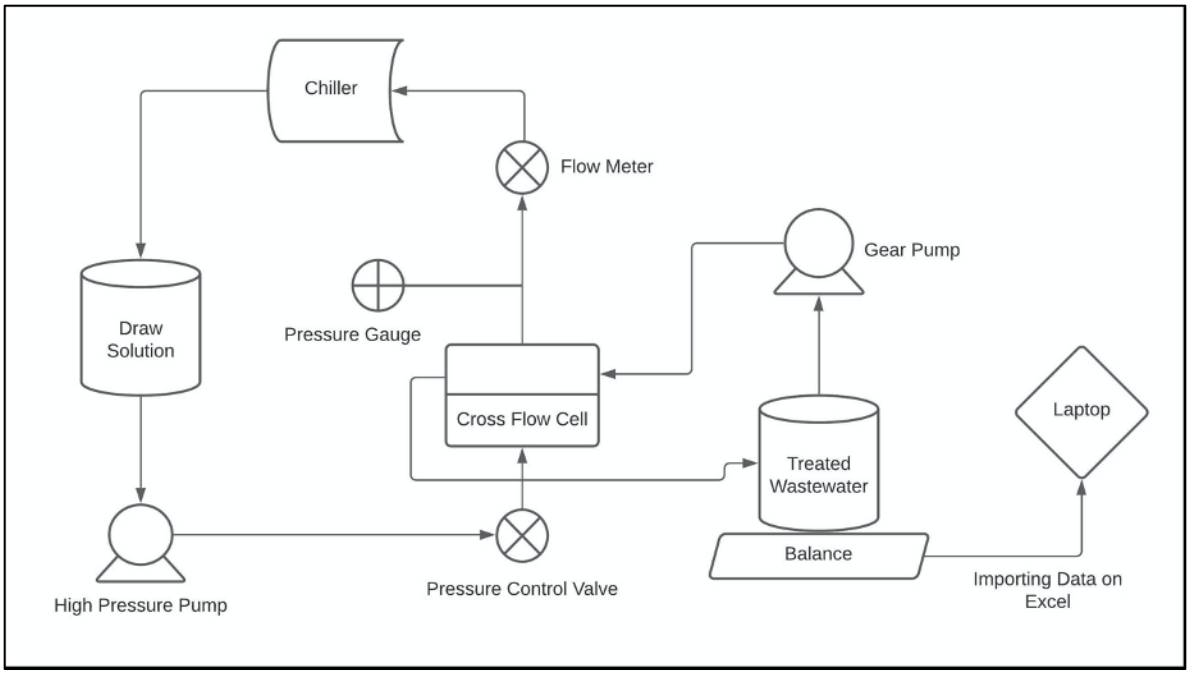

Figure 8: Schematic of PRO experiment

Chapter 4: Results and Discussion

4.1 Characterization Results of Analyses

The results from IC and ICP-MS tests for the raw wastewater, are shown in Tables 5 and 6. As illustrated in the tables, the concentration of sulfate is much higher than the other ions due to the use of sulfuric acid in the leaching process to absorb gold and other metals in the gold ore. A high concentration of sulfate could be problematic because, this ion can precipitate with metal cations and causes scaling. A high concentration of copper and magnesium can lead to reaction with sulfate ions, and scaling and performance reduction. In addition to that, high concentrations of sodium and magnesium ions which are probably due to addition of sodium hydroxide and magnesium hydroxide in the neutralisation process, are concerning which leads to elevated concentrations of these ions in the retentate and fouling on the NF membrane surface (explained in NF section). This effluent with moderately high amounts of TOC, can promote organic fouling on the UF membrane surface, leading to flux and water recovery reduction.

Table 5: The concentration of the ions by IC analysis

Ion	Cl^-	NO_2^-	NO_3^-	SO_4^{2-}	Na^+	NH_4^+	K^+	Ca^{2+}	Mg^{2+}	TOC	pH
Concentration (mg/L)	177.4	74.5	141.5	3337.4	690.6	145.9	87.0	19.3	574.6	10.7	5.5

Table 6: The concentration of the heavy metals by ICP-MS analysis

Element	Al	Cr	Mn	Fe	Co	Ni	Cu	Zn	As	Se	Cd	Sb	Pb
Concentration (µg/L)	8.2	0.5	6.5	0.0	12.5	2.8	210.2	64.7	1.0	167.7	0.1	6.9	1.8

4.2 Ultrafiltration Experiment

The UF process is necessary for reducing the colloids and smaller suspended solids which were not separated using the MF filter in the first place, as well as macromolecules and high molecular weight organic matter. This application will lead to fouling reduction in NF, reduced damage to the module, membrane lifetime increase, improved separation performance and higher water quality in NF. Moreover, UF not only produces high quality permeate for NF but also, it does not require sludge treatment. Thus, the need for equipment maintenance and repair and sludge discharge will be less which reduces operational cost substantially. According to Andrade et al. [97], the application of UF prior to NF increased the solid removal efficiency and permeate flux in the NF. The average achieved water flux for UF was 123.0 $\pm$ 7.4 LMH. Using equation 7, the water recovery over 6 hours was 60%. The permeate flux for UF process is shown in Figure 9.

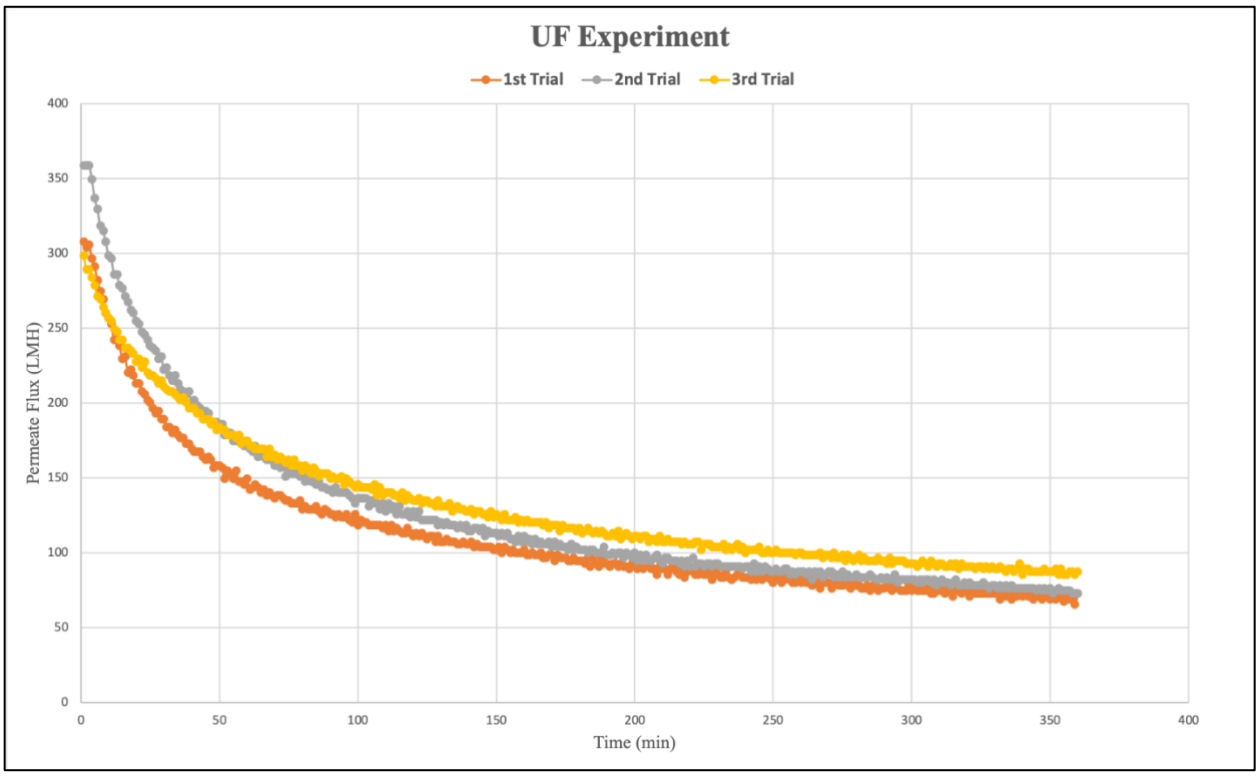

Figure 9: UF permeate flux

According to Figure 9, the water flux reduces over time due to the fouling effect. As the process goes on, the feed solution pH increases which leads to salt and metal precipitation. This phenomenon increases the concentration of the suspended solids in the solution. Consequently, accumulation of solids on the membrane surface and concentration polarization occurs [98]. As it is noted in Table 7, the magnesium ion concentration in the retentate reduces much more compared to other ions which proves the precipitation of $Mg(OH)_2$ on the membrane surface. Moreover, as mentioned in the previous section, sulfate can react with metal cations and cause scaling, leading to water flux reduction. Considering the amount of sulfate scaled on the membrane, it can be concluded that scaling might happen due to sulfate reactions with metal cations such as magnesium and sodium. At the end of the test, when the membrane was removed from the cell, it was observed that white solids precipitated on the membrane. According to mass balance calculations, the precipitate solids on membrane surface are mostly sulfate, magnesium and sodium. In addition to that, organic materials existing in the feed solution can reduce UF performance by blocking the membrane surface. The results for IC and ICP-MS analyses are illustrated in Tables 7 and 8. The findings from the mass calculation are illustrated on the third row of Table 7.

Table 7: Concentration of the ions by IC analysis

Ion	$\mathbf{Cl^-}$	$\mathbf{NO_2^-}$	$\mathbf{NO_3^-}$	$\mathbf{SO_4^{2-}}$	$\mathbf{Na^+}$	$\mathbf{NH_4^+}$	$\mathbf{K^+}$	$\mathbf{Ca^{2+}}$	$\mathbf{Mg^{2+}}$	**pH**
Retentate (mg/L)	169	55.2	140.1	3109.2	665.9	144.4	87.0	13.9	402.7	8.8
Permeate (mg/L)	158.2	53.4	125.8	2963.9	586.3	135.6	82.1	13.0	438.2	8.5
On membrane surface (mg)	70.1	101.2	44.2	1518.8	330.5	30.4	132.1	29.3	767.2	-

Table 8: The concentration of the heavy metals by ICP-MS analysis

Element	Al	Mn	Co	Ni	Cu	Zn	Se	Sb
Permeate (µg/L)	5.9	5.5	11.7	2.5	177.4	55.4	158.6	5.8

4.3 Nanofiltration Experiment

The purpose of the NF process is to remove the ions, metalloids, heavy metals, and organic foulants prior to the PRO process. The NF permeate will be implemented in PRO as the feed solution. Therefore, it must remove the foulants as much as possible to prevent fouling in the FO membrane support layer. Also, the lower the level of solids in the NF permeate, the higher the driving force (difference in osmotic pressure across the membrane) in PRO because, produced osmotic pressure in the feed side will be minimal. The permeate flux from this process is illustrated in Figure 10. The average achieved water flux was 49.5 $\pm$ 2.5 LMH under 300 psi after 6 hours of operation. The water recovery was observed to be around 28%. Compared to UF, the NF membrane has much lower pore size and tighter (300 Da Vs. 20 kDa) which explains the much lower water recovery. This membrane can withstand pressures up to 600 psi but due to the setup limitations the applied pressure was set at 300 psi. By increasing the applied pressure and controlling the foulants, higher water fluxes and water recoveries can be achieved.

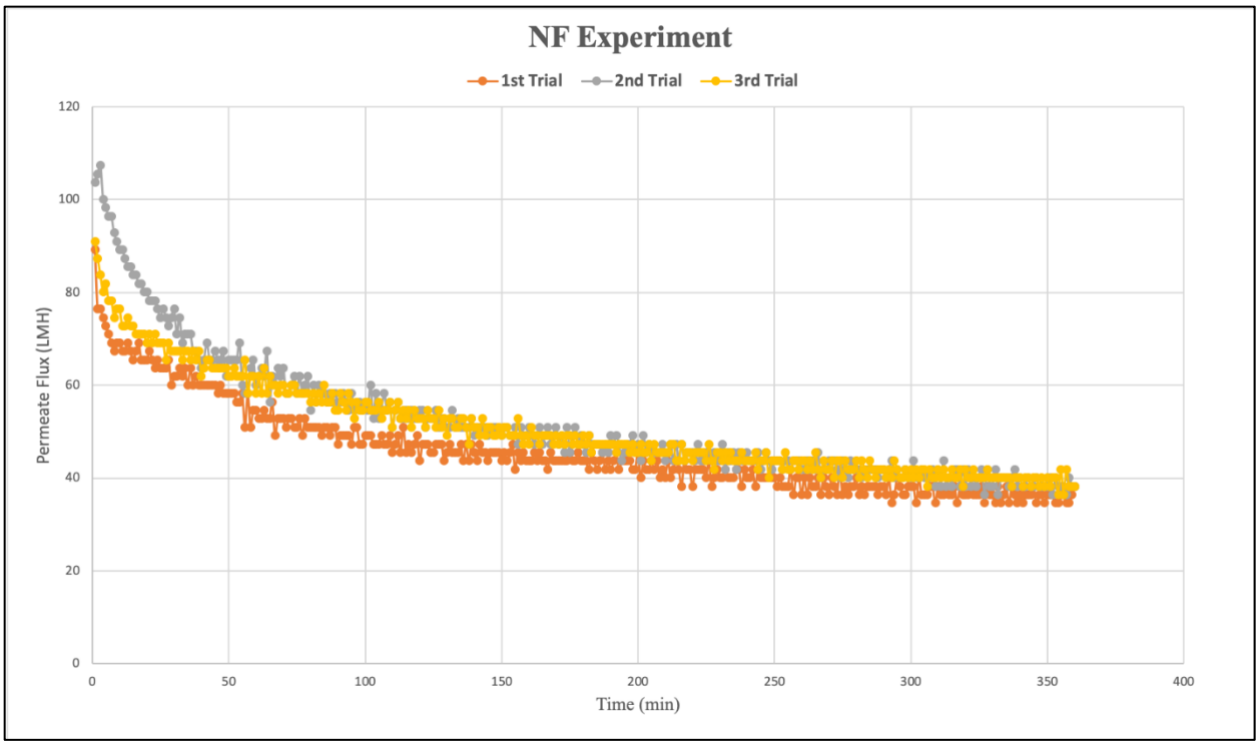

Figure 10: NF permeate flux over time

An increase in temperature leads to reduction in the separation performance of NF due to increased pore size in the membrane [96]. Therefore, in the experiments the temperature was maintained at 20°C. It was observed that the permeate flux diminished drastically due to the fouling effect. According to the IC result, ions such as Na^{+} and Mg^{2+} most likely caused severe fouling on the membrane surface leading to water flux reduction and low recovery. According to a previous study, pH above 6.0 increases the scaling potential in gold mining solution [97]. The NF retentate pH is high which causes the membrane surface to be negatively charged, and forms complexes with abundant cations in the solution [99]. It was observed that the NF membrane rejection towards sulfate is high due to its hydrated size and divalent charge. On the contrary, the retention efficiency for chloride and sodium are not as high as sulfate. These ions have a smaller hydrated radius and are monovalent. In addition to that, charged membranes repel high-valence ions more at higher pH [100]. Another reason for the water flux reduction is that as the filtration

proceeds, the concentration of ions in the retentate increases due to rejection of solutes and passing the water by the NF membrane. This will lead to an increase in osmotic pressure in the solution and membrane surface. Since the difference between osmotic pressure and applied pressure is the driving force in this process, water flux reduction happens when the applied pressure is constant [102]. The results from characterization analyses are shown in Tables 9 and 10. In these tables, total removal efficiency (comparison of initial wastewater and NF permeate) is included to determine the pre-treatment processes effectiveness. According to the results, it can be concluded that the NF process produced high-quality permeate that can be circulated back to the main process for reuse.

Table 9: Concentration of the ions by IC analysis

Ion	$\mathbf{Cl^-}$	$\mathbf{NO_2^-}$	$\mathbf{NO_3^-}$	$\mathbf{SO_4^{2-}}$	$\mathbf{Na^+}$	$\mathbf{NH_4^+}$	$\mathbf{K^+}$	$\mathbf{Ca^{2+}}$	$\mathbf{Mg^{2+}}$	**pH**
Retentate (mg/L)	158.0	51.3	101.6	3077.1	611.5	174.7	81.7	13.3	421	8.6
Permeate (mg/L)	3.6	7.8	17.2	24.5	32.5	19.0	8.1	1.8	35.0	8.0
Total Removal Efficiency (%)	98	90	88	99	95	87	91	91	94	-

Table 10: Concentration of the heavy metals by ICP-MS analysis

Element	**Al**	**Mn**	**Co**	**Ni**	**Cu**	**Zn**	**Se**	**Sb**
Permeate (µg/L)	1.6	< 1	< 1	< 1	8.9	6.3	1.9	1.0
Total Removal Efficiency (%)	81	~100	~100	~100	86	90	99	86

4.4 Pressure Retarded Osmosis Experiments

The purpose of the PRO process is to generate electricity, utilizing water pretreated by the NF process as the feed solution. The NF permeate total dissolved solids (TDS) is not high. Therefore, its generated osmotic pressure is not high which makes it a good candidate for PRO application. The average achieved permeate flux and water recovery was 43.5 $\pm$ 1.1 LMH and 28%, respectively, over 6 hours. As it is shown in Figure 11, the permeate flux decreases gradually over time. Since the membrane is not ideal and its salt rejection is not 100%, salt diffusion through the membrane's active layer (facing the draw solution) will happen due to concentration difference across the membrane. This reverse flux will cause accumulation and scaling of the draw solutes in the membrane support layer, leading to ICP which reduces the effective driving force across the membrane, and consequently, the water flux [103]. The calculated RSF using equation 9 was 3.9 $g/m^2.h$ (gMH). Compared to inorganic salts, the RSF is higher due to smaller hydrated ion size [23]. Also, ammonia is a nutrient and may promote biofouling on the feed side of the membrane [32], which leads to water flux reduction. The generated power densities are illustrated in Figure 12 with the average of 15.0 $\pm$ 0.4 W/m^2. According to a previous study [104], for the PRO plant to be profitable, the power density should range between 4-6 W/m^2. Therefore, the achieved power density using treated wastewater, which was investigated in this study, showed a promising result. In another test, DI water was used as the feed solution to evaluate the fouling effect of the wastewater in membrane support layer. As illustrated in Figures 11 and 12, the water flux and power density are higher in this case. The achieved water flux and generated power were 64.2 LMH and 22.2 W/m^2 which clearly shows the detrimental effect of fouling. In the draw side, the hydrodynamic shear force induced by cross-flow prevents solute deposition on the active layer of the membrane. However, in the support layer, there is no shear force and, thus, solute deposition

causes a severe flux decline. Kim et al. [105] investigated the fouling propensity of organic and inorganic matter in the membrane support layer and concluded that the inorganic scaling has a superior effect on flux reduction compared to the organic one. According to Table 9, the NF permeate (feed solution) mostly contains sulfate, sodium and magnesium ions which can be responsible for the scaling and ICP. Hydrodynamic cleaning is unsuccessful in inorganic fouling mitigation while, the implementation of anti-scalant showed effective results [105]. Compared to previous studies, the proposed system generated higher power density. Wan and Chung [21] reported the power density of 8.9 W/m^2 using NF for pre-treating the wastewater. In their experiments SWRO from RO plant utilized as the draw solution. Sakai et al. [92] investigated the utilization of Fukuoka SWRO brine and treated sewage as the draw and feed solutions, respectively. According to their study, the maximum power density for the system using 10-in modules was 13.5 W/m^2. Therefore, the proposed system has good potential to compete other proposed systems.

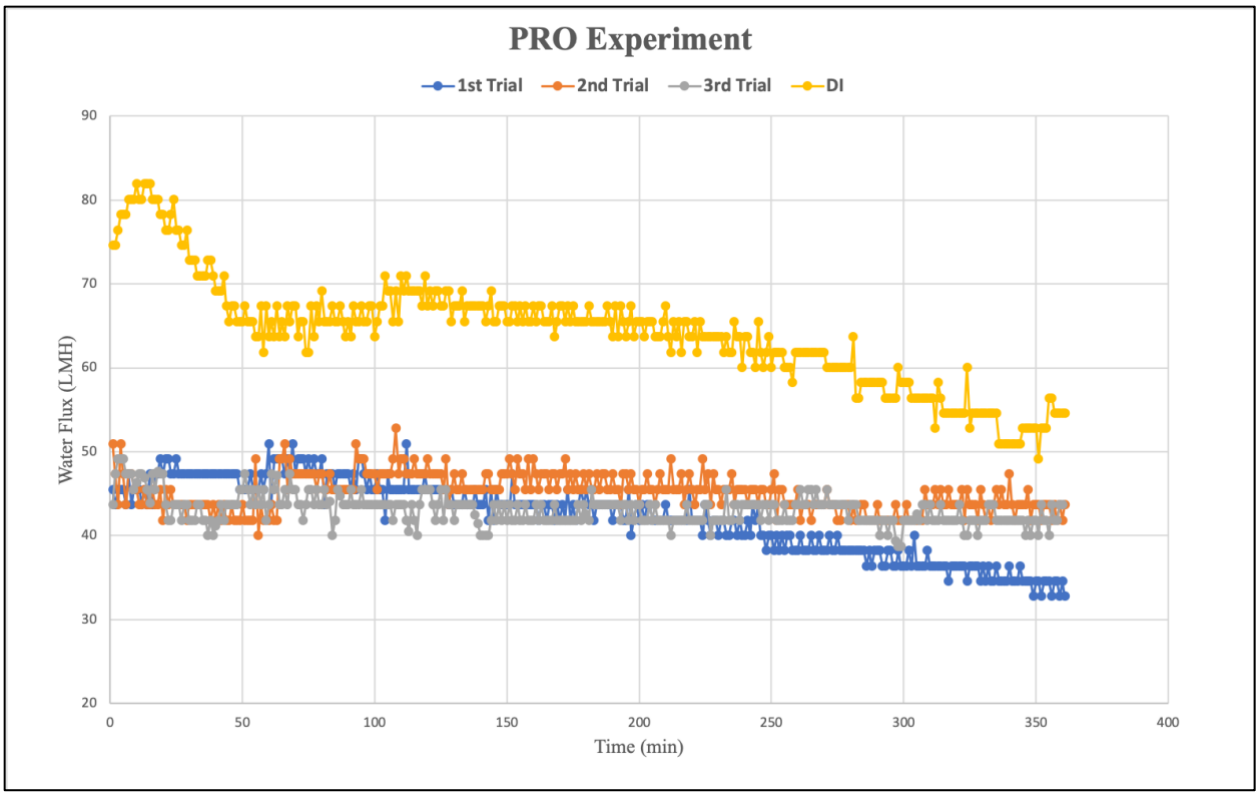

Figure 11: PRO permeate flux

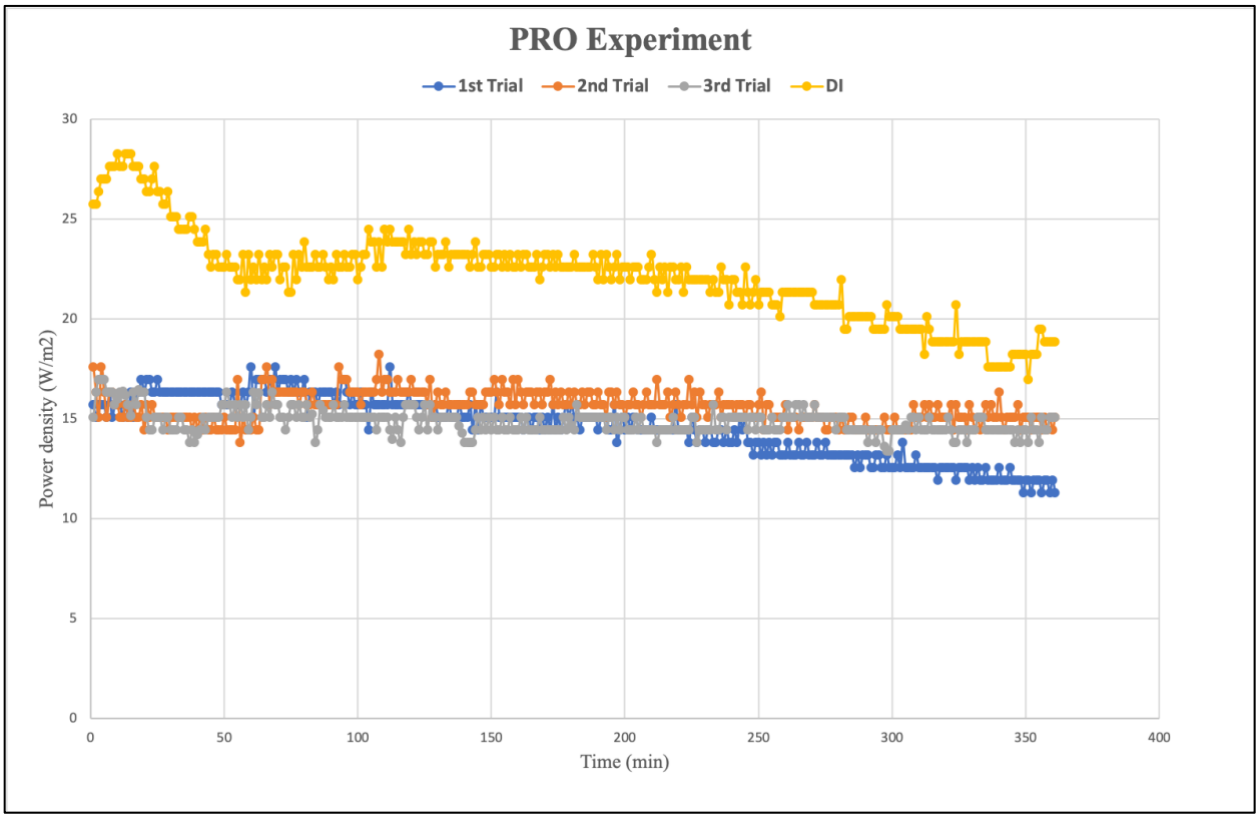

Figure 12: Generated power density by PRO

4.5 Thermal Efficiency and Energy Consumption of the Osmotic Heat Engine

As the water permeates through the membrane, the draw solution becomes diluted and the osmotic gradient across the membrane decreases which, consequently, reduces the water flux. Thus, the diluted draw solution must be re-concentrated in the recovery unit after electricity generation and circulated back to the system again. The permeated water is separated from the draw solutes using one of the techniques described in section 2.5. A single distillation column is a suitable unit for separating ammonia and carbon dioxide to produce water and concentrated draw solution. According to a study by McGinnis et al. [27], this separation can be done by utilizing low-grade heat with the temperature of 50℃. They calculated all the heat and electrical duties for recovering 3M solution using HYSIS® chemical simulation model. Based on their modeling, the heat and electrical duties are 865.7 MJ/m^3 and 0.16 MJ/m^3 (per m^3 of working fluid produced containing <1 ppm NH_3). It is clear that electrical duty is negligible compared to the heat one. Multiplying the heat duty by the average water flux (43.5 LMH) that is achieved in this study, the required heat will be 10.5 kW/m^2. The thermal efficiency of this process is defined as the ratio of power generated in PRO to the heat and electrical duties for re-concentrating the diluted draw solution in the recovery unit. Consequently, the thermal efficiency of the OHE is significantly low (0.14%) which is in the range that was predicted by another study [51]. The engine efficiency can be improved by implementing waste heat at temperature of 100℃. Moreover, draw solutions with higher concentration (up to 6M) can increase the water flux remarkably which requires less membrane area and lowers the membrane cost. Theoretically, the water flux can be calculated using the following equation [77]:

$$J = A(\Delta\pi - \Delta P) \quad (8)$$

Where A is the water permeability coefficient ($^{m^3}/_{m^2.s.pa}$) and $\Delta\pi$ is osmotic pressure difference between feed and draw solutions. Substituting this equation into Equation 7 and differentiating power density with respect to ΔP, the maximum power density is achievable when the applied pressure is half of the difference of osmotic pressure across the membrane. This draw solution at 3M concentration can produce osmotic pressure more than 1700 psi [27]. Since the feed solution osmotic pressure is negligible, therefore, in order to achieve the draw solution full potential, an applied pressure of 850 psi is needed. In our experiment, the membrane's maximum operational pressure was 180 psi which is far from the desired applied pressure. Therefore, the generated power density can be around 75 W/m^2 [27] which will result in a thermal efficiency of 0.7%. However, increasing ΔP will increase the RSF which lowers the process efficiency. Also, higher applied pressures need special equipment and more energy consumption which increase both the capital and operational costs. Thus, a trade-off should be done to optimize its performance.

Chapter 5: Conclusions and Recommendations

In the last decade, SG has been widely studied as a potential source of energy that can be harvested using PRO which has shown promising results. In this study, the feasibility of implementing mining wastewater as the feed solution in CLPRO to generate electricity was investigated. In the pre-treatment step, UF was used to reduce colloids and macromolecules and organic fouling propensity. In the NF step, TDS and heavy metals was removed significantly from the wastewater. The results showed that removal efficiency is high, and the concentration of the comprising ions and heavy metals reduced to an acceptable amount. However, the fouling effect leads to a great flux and water recovery decline. It seems that the optimum pH for pre-treatment processes is below 5.0 [97]. Therefore, maintaining the pH in this range as well as using the anti-scalant can effectively increase the separation performance. In PRO a steady water flux trend (43.5 LMH) and power density of $15.0 \pm 0.4\ \mathrm{W/m^2}$ after 6 hours was achieved which shows promising results for future large-scale applications.

Overall, to our knowledge this study is the first one which investigated gold mining wastewater as the feed solution in PRO. The wastewater has a great potential to be implemented as the feed water in PRO. The pre-treatment processes showed remarkable effectiveness in treating the wastewater and reducing the TDS to the acceptable degree. Fouling components such as sulfate, sodium and magnesium play the main role in the fouling propensity of the membrane processes. The PRO system generated remarkably high power density compared to the previous studies on wastewater. The regeneration unit can reconcentrate the diluted draw solution using waste heat with an acceptable thermal efficiency. However, the efficiency of the osmotic engine can be improved by utilizing LGH at higher temperatures (up to 100℃), a draw solution at higher concentrations (up

to 6 M) and higher applied pressures which is half of the generated osmotic pressure by the draw solution (1700 psi).

Future work should focus on fouling mitigation which results in operational and membrane cost reduction and enhanced separation performance. The most crucial issue in CLPRO is the membrane. Improving membrane selectivity as well as its mechanical strength (up to 100 bars) should be focused on and studied by research groups. Developing membranes with thinner support layers and higher porosity and robustness at the same time, can make this process viable. Applying more pressure on the membrane makes it possible to harvest the full potential of draw solutions which leads to higher power densities. Improved membrane selectivity and porosity can lower RSF and ICP significantly. Also, different draw solutes such as NaCl can be investigate in this system. Furthermore, there are several methods to assess productivity, efficiency, envirosafety, and sustainability of an energy system such as life-cycle assessment (LCA), techno-economic analysis, emergy analysis, energy analysis, and exergy analysis. It was concluded that among the methods mentioned, exergy analysis is the most effective one [78]. Exergy analysis not only evaluates the quantity of the energy streams but also, the quality of them. This method considers both first and second laws of thermodynamic, and through assuming reversible processes it determines the maximum achievable work a thermodynamic system can generate until it reaches the equilibrium state. Furthermore, this method can be integrated with environmental and economic concepts which are known as exergoenvironmental and exergoeconomic. By applying thermodynamic limits, this assessment can show precisely economic and energy losses to assess the sustainability of a system. Therefore, future work should investigate PRO under exergy analysis and to be specific exergoeconoenvironmental assessment which proposed by Aghbashlo and Rosen [79] to quantify the efficiency of the system, LCOE, envirosafety and sustainability.

References

[1] J. E. Cohen, "Human Population: The Next Half Century," *Science*, vol. 302, no. 5648, pp. 1172-1175, Nov. 2003.

[2] IEA. World energy outlook; 2019, https://iea.blob.core.windows.net/assets/98909c1b-aabc-4797-9926-35307b418cdb/WEO2019-free.pdf

[3] H. K. S. Panahi, M. Dehhaghi, K. E. Kinder, T. C. Ezeji, "A review on green liquid fuels for the transportation sector: a prospect of microbial solutions to climate change," *Biofuel Res. J.,* vol. 23, pp. 995-1024, Sep. 2019.

[4] D. Gielen, F. Boshell, D. Saygin, M. D. Bazilian, N. Wagner, R. Gorini, "The role of renewable energy in the global energy transformation," *Energy Strategy Reviews,* vol. 24, pp. 38-50, Apr. 2019.

[5] U.S. Energy Information Administration, https:/www.eia.gov/energyexplained/renewable-sources

[6] M. B. Hayat, D. Ali, K. C. Monyake, L. Alagha, N. Ahmed, "Solar energy—A look into power generation, challenges, and a solar-powered future," *Int. J. Energy Res.*, vol. 43, pp. 1049-1067, Nov. 2018.

[7] R. Mckenna, P. O. Leye, W. Fichtner, "Key challenges and prospects for large wind turbines," *Renewable and Sustainable Energy Reviews,* vol. 53, pp. 1212-1221, Jan. 2016.

[8] A.Tursi, "A review on biomass: importance, chemistry, classification, and conversion," *Biofuel Res. J.*, vol.22, pp. 962-979, June 2019.

[9] K. Touati K and F. Tadeo, "Green energy generation by pressure retarded osmosis: State of the art and technical advancement," *Int. J. Green Energy*, vol. 14, pp. 337–360, Nov. 2016.

[10] R. E. pattle, “Production of electric power by mixing fresh water and saltwater in the hydroelectric pile,” *Nature*, vol. 174, pp. 660, Oct. 1954.

[11] N. Y. Yip and M. Elimelech, “Comparison of energy efficiency and power density in pressure retarded osmosis and reverse electrodialysis,” *Environ. Sci. Technol.,* vol. 48, pp. 11002−11012, Aug. 2014.

[12] F. Calise, M. D. D’accadia, M. Santarelli, A. Lanzini, D. Ferrero, “Solar Hydrogen Production, Processes, Systems and Technologies,” *Academic Press*, ISBN 978-0-12-814853-22019, 237-95.

[13] S. J. Zarrouk and H. Moon, “Efficiency of geothermal power plants: A worldwide review,” *Geothermics*, vol. 51, pp. 142-153, July 2014.

[14] A. K. Gupta, “Efficient Wind Energy Conversion: Evolution to Modern Design,” *J. Energy Resour. Technol.*, vol. 137, pp. 051210, Sep. 2015.

[15] X. Liu, Z. Chen, Y. Si, P. Qian, H. Wu, L. Cui, D. Zhang, “A review of tidal current energy resource assessment in China,” *Renewable and Sustainable Energy Reviews,* vol. 145, pp. 111012, July 2021.

[16] I. Yukse, “As a renewable energy hydropower for sustainable development in Turkey,” *Renewable and Sustainable Energy Reviews,* vol. 14, pp. 3213-3219, Dec. 2010.

[17] S. Lin, A. P. Straub, M. Elimelech, “Thermodynamic limits of extractable energy by pressure retarded osmosis,” *Energy Environ. Sci.*, vol. 7, pp. 2706-2714, May 2014.

[18] S. Loeb, “Energy production at the Dead Sea by pressure retarded osmosis: Challenge or chimera,” *Desalination*, vol. 120, pp. 247–262, Dec. 1998.

[19] S. Loeb, “One hundred and thirty benign and renewable megawatts from Great Salt Lake? The possibility of hydroelectric power by pressure retarded osmosis,” *Desalination*, vol. 141, pp. 85–91, Dec. 2001.

[20] N. Y. Yip and M. Elimelech, “Thermodynamic and energy efficiency analysis of power generation from natural salinity gradients by pressure retarded osmosis,” *Environ. Sci. Technol.*, vol. 141, pp. 5230–5239, Apr. 2012.

[21] C. F. Wan and T. Chung, “Osmotic power generation by pressure retarded osmosis using seawater brine as the draw solution and wastewater retentate as the feed,” *J. Membr. Sci.,* vol. 479, pp. 148-158, Apr. 2015.

[22] A. Achilli, T. Y. Cath, A. E. Childress, “Selection of in organic-based draw solutions for forward osmosis applications,” *J. Membr. Sci.*, pp. 233-241, Nov. 2010.

[23] Md. S. Islam, S. Sultana, S. Adhikary, Md. S. Rahaman, “Highly effective organic draw solutions for renewable power generation by closed-loop pressure retarded osmosis,” *Energy Conversion and Management*, pp. 1226-1236, Sep. 2018.

[24] G. Han, Q. Ge, T. Chung, “Conceptual demonstration of novel closed-loop pressure retarded osmosis process for sustainable osmotic energy generation,” *Applied Energy*, pp. 3833-93, Nov. 2014.

[25] D. D. Anastasio, J. T. Arena, E. A. Cole, J. R. McCutcheon, “Impact of temperature on power density in closed-loop pressure retarded osmosis for grid storage,” *J. Membr. Sci.*, vol. 479, pp. 240–245, Apr. 2015.

[26] E. Shaulsky, C. Boo, S. Lin, M. Elimelech, “Membrane-Based Osmotic Heat Engine with Organic Solvent for Enhanced Power Generation from Low-Grade Heat,” *Environ. Sci. Technol.*, vol. 49, pp. 5820−5827, Apr. 2015.

[27] R. L. McGinnis, J. R. McCutcheon, M. Elimelech, "A novel ammonia–carbon dioxide osmotic heat engine for power generation," *J. Membr. Sci.*, vol. 305, pp. 13–19, Nov. 2007.

[28] K. L. Hickenbottom, J. Vanneste, T. Y. Cath, "Assessment of alternative draw solutions for optimized performance of a closed-loop osmotic heat engine," *J. Membr. Sci.*, vol. 504, pp. 162-175, Apr. 2016.

[29] H. Gong, D. D. Anastasio, K. Wang, J. R. McCutcheon, "Finding better draw solutes for osmotic heat engines: Understanding transport of ions during pressure retarded osmosis," *Desalination*, vol. 421, pp. 32–39, Nov. 2017.

[30] S. Lin, N. Y. Yip, T. Y. Cath, C. O. Osuji, M. Elimelech, "Hybrid pressure retarded o–osis--membrane distillation system for power generation from low-grade heat: Thermodynamic analysis and energy efficiency," *Environ. Sci. Technol.*, vol. 48, 5306-5313, Apr. 2014.

[31] S. J. Moon, J. H. kim, J. G. Seong, W. H. Lee, S. H. Park, S. H. Noh, et al., "Thin film composite fluorinated thermally rearranged polymer nanofibrous membrane achieves power density of 87 W/m^2 in pressure retarded osmosis, improving economics of osmotic heat engine," *J. Membr. Sci.*, vol. 607, pp. 118120, Jul. 2020.

[32] Q. She, Y. K. W. Wong, S. Zhao, C. Y. Tang, "Organic fouling in pressure retarded osmosis: experiments, mechanisms and implications," *J. Membr. Sci.*, vol. 428, pp. 181-189, Feb. 2013.

[33] K. Touati, C. Hanel, F. Tadeo, T. Schiestel, "Effect of feed and draw solution temperatures on PRO performance: Theoretical and experimental study," *Desalination,* vol. 365, pp. 182-195, June 2015.

[34] K. L. Hickenbottom, J. Vanneste, M. Elimelech, T. Y. Cath, "Assessing the current state of commercially available membranes and spacers for energy production with pressure retarded osmosis," *Desalination*, vol. 389, pp. 108-118, July 2016.

[35] P. G. Jessop, D. J. Heldebrant, X. Li, C. A. Eckert, C. L. Liotta, “Green chemistry: reversible nonpolar-to-polar solvent” *Nature*, vol. 436, pp. 1102, Aug. 2005.

[36] L. Phan, J. R. Andreatta, L. K. Horvey, C. F. Edie, A. Luco, A. Mirchandani, et al., “Switchable-polarity solvents prepared with a single liquid component,” *J. Org. Chem.*, vol. 73, 127–132, Dec. 2007.

[37] P. Pollet, C. A. Eckert, C. L. Liotta, “Switchable solvents,” *Chem. Sci.*, vol. 2, pp. 609–614, 2011.

[38] P. G. Jessop, S. M. Mercer, D. J. Heldebrant, “CO_2-triggered switchable solvents, surfactants, and other materials,” *Energy Environ. Sci.*, vol. 5, 7240–7253, Feb. 2012.

[39] M. M. Ling and T. S. Chung TS, “Desalination process using super hydrophilic nanoparticles via forward osmosis integrated with ultrafiltration regeneration,” *Desalination*, vol. 278, pp. 194-202, Sep. 2011.

[40] R. L. McGinnis, “Osmotic desalination process,” *US Patent*, 2002.

[41] M. L. Stone, C. Rae, F. F. Stewart, A. D. Wilson, “Switchable polarity solvents as draw solutes for forward osmosis,” *Desalination*, vol. 312, pp. 124-129, Mar. 2013.

[42] D. J. Johnson, W. A. Suwaileh, A. W. Mohammed, N. Hilal, “O’motic's potential: An overview of draw solutes for forward osmosis,” *Desalination*, vol. 434, pp. 100–120, May 2018.

[43] R. L. McGinnis RL and M. Elimelech, “Energy requirements of ammonia–carbon dioxide forward osmosis desalination,” *Desalination*, vol. 207, pp. 370–382, Mar. 2007.

[44] O. J. Morin, “Design and operating comparison of MSF and MED systems,” *Desalination*, vol. 93, pp. 69-109, Aug. 1993.

[45] Adham S, Hussain A, Matar JM, Dores R, Janson A. "Application of membrane distillation for desalting brines from thermal desalination plants," *Desalination*, vol. 314, pp. 101–108, Apr. 2013.

[46] P. Wang and T. S. Chung, "A conceptual demonstration of freeze desalination–membrane distillation (FD–MD) hybrid desalination process utilizing liquefied natural gas (LNG) cold energy" *Water Res.,* vol. 46, pp. 4037–4052, Sep. 2012.

[47] D. L. Shaffer, L. H. A. Chavez, M. Ben-Sasson, S. R. V. S. Castrillón, N. Y. Yip, M. Elimelech, "Desalination and reuse of high-salinity shale gas produced water: Drivers, technologies, and future directions," *Environ. Sci. Technol.,* vol. 47, pp. 9569-9583, Jul. 2015.

[48] C. Bier and U. Plantikow, "Solar powered desalination by membrane distillation," *IDA World Congress on Desalination and Water Science - Abu Dhabi*, pp. 397–410, 1995.

[49] J. Koschikowski, M. Wieghaus, M. Rommel, "Solar thermal-driven desalination plants based on membrane distillation," *Desalination*, vol. 156, pp. 295–304, Aug. 2003.

[50] M. S. El-Bourawi, Z. Ding, R. Ma, M. Khayet, "A framework for better under- standing membrane distillation separation process," *J. Membr. Sci*., vol. 285, pp. 4–29, Nov. 2006.

[51] K. L. Hickenbottom, J. Vanneste, L. Miller-Robbie, A. Deshmukh, M. Elimelech, M. B. Heeley, T. Y. Cath TY, "Techno-economic assessment of a closed-loop osmotic heat engine." *J. Membr. Sci.,* vol. 535, pp. 178–187, August 2017.

[52] U.S. Energy Information Administration, *Wholesale Electricity and Natural Gas Market Data* https://www.eia.gov/electricity/wholesale/, 2015.

[53] S. Quoilin, M. V. D. Broek, S. Declaye, P. Dewallef, V. Lemort, "Techno-economic survey of Organic Rankine Cycle (ORC) systems," *Renew. Sustain. Energy Rev.*, vol. 22, pp. 168–186, June 2013.

[54] R. Vescovo, "ORC recovering industrial–heat - power generation from waste energy streams, Cogeneration and on-site power production," http://www.decentralized-energy.com/articles/print/volume-10/issue-2/features/orcrecovering-industrial-heat-power-generation-from-waste-energy-streams.html, Apr. 2009.

[55] S. Lin, N. Y. Yip, T. Y. Cath, C.O. Osuji, M. Elimelech, "Hybrid pressure retarded osmosis-membrane distillation system for power generation from low-grade heat: Thermodynamic analysis and energy efficiency." *Environ. Sci. Technol.*, vol. 48, pp. 5306-5313, Apr. 2014.

[56] C. F. Wan and T. Chung, "Techno-economic evaluation of various RO+PRO and RO+FO integrated processes," *Applied Energy*, vol. 212, pp. 1038-1050, Feb. 2018.

[57] Q. Wang, Z. Zhou, J. Li, Q. Tang, Y. Hu, "Investigation of the reduced specific energy consumption of the RO-PRO hybrid system based on temperature-enhanced pressure retarded osmosis," *J. Membr. Sci*., vol. 581, pp. 439-452, July 2019.

[58] J. L. Prante, J. A. Ruskowitz, A. E. Childress, A. Achilli, "RO-PRO desalination: an integrated low-energy approach to seawater desalination," *Applied Energy,* vol. 120, pp. 104-114, May 2014.

[59] C. F. Wan and T. S. Chung, "Energy recovery by pressure retarded osmosis (PRO) in SWRO–PRO integrated processes," *Applied Energy*, vol. 162, pp. 687-698, Jan. 2016.

[60] B. Blankert, Y. Kim, H. Vrouwenvelder, N. Ghaffour, "Facultative hybrid RO-PRO concept to improve economic performance of PRO: Feasibility and maximizing efficiency," *Desalination*, vol. 478, pp. 114268, Mar. 2020.

[61] M. Elimelech and W. A. Phillip, "The future of seawater desalination: energy, technology, and the environment," *Science*, vol. 333, pp. 712-717, Aug. 2011.

[62] A. M. Delgado-Torres and L. Garcia-Rodriguez, "Status of solar thermal-driven reverse osmosis desalination," *Desalination*, vol. 216, pp. 242-251, Oct. 2007.

[63] A. Maleki, M. G. Khajeh, M. A. Rosen, "Weather forecasting for optimization of a hybrid solar-wind-empowered reverse osmosis water desalination system using a novel optimizer approach," *Energy,* vol. 114, pp. 1120-1134, Nov. 2016.

[64] A. Maleki, "Design and optimization of autonomous solar-wind-reverse osmosis desalination systems coupling battery and hydrogen energy storage by an improved bee algorithm," *Desalination*, vol. 435, pp. 221-234, June 2018.

[65] D. A. Dehmas, N. Kherba, F. B. Hacene, N. K. Merzouk, M. Merzouk, H. Mahmoudi, M. F. Goosen, "On the use of wind energy to power reverse osmosis desalination plant: a case study from Tenes (Algeria)," *Renew. Sustain. Energy Rev.*, vol. 15, pp. 956-963, Feb. 2011.

[66] W. He, Y. Wang, M. H. Shaheed, "Stand-alone seawater RO (reverse osmosis) desalination powered by PV (photovoltaic) and PRO (pressure retarded osmosis)," *Energy*, vol. 86, pp. 423-435, June 2015.

[67] X. Tong, S. Liu, Y. Chen, J. Crittenden, "Thermodynamic analysis of a solar thermal facilitated membrane seawater desalination process," *J. Clean. Prod.*, vol. 256, pp. 120398, May 2020.[68] R. Alnaizy, A. Aidan, M. Qasim, "Draw solute recovery by metathesis precipitation in forward osmosis desalination," *Desalination and Water Treatment*, vol. 51, pp. 5516-5525, Mar. 2013.

[69] R. Alnaizy, A. Aidan, M. Qasim, "Copper sulfate as draw solute in forward osmosis desalination," *J. Environ. Chem. Eng.*, vol. 1, pp. 424–430, Sep. 2013.

[70] H. Luo, Q. Wang, T. C. Zhang, T. T. A. Zhou, L. Chen, X. Bie, "A review on the recovery methods of draw solutes in forward osmosis," *Journal of Water Process Engineering*, vol. 4, pp. 212–223, Dec. 2014.

[71] G. D. Moeser, K. A. Roach, W. H. Green, T. A. Hatton, "High-gradient magnetic separation of coated magnetic nanoparticles," *AIChE*, vol. 50, pp. 2835, Oct. 2004.

[71] K. Touati, H. S. Usman, C. N. Mulligan, Md. S. Rahaman, "Energetic and economic feasibility of a combined membrane-based process for sustainable water and energy systems," *Apply Energy*, vol. 264, pp. 114699, Apr. 2020.

[72] H. W. Chung, L. D. Banchik, J. Swaminathan, V. J. H. Lienhard, "On the present and future economic viability of standalone pressure-retarded osmosis," *Desalination*, vol. 408, pp. 133–144, Apr. 2017.

[73] H. W. Chung, J. Swaminathan, L. D. Banchik, J. H. Lienhard, "Economic framework for net power density and levelized cost of electricity in pressure-retarded osmosis," *Desalination*, vol. 448, pp. 13–20, Dec. 2018.

[74] K. Touati and Md. S. Rahaman, "Viability of pressure-retarded osmosis for harvesting energy from salinity gradients," *Renewable and Sustainable Energy Reviews*, vol. 131, pp. 109999, Oct. 2020.

[75] A. P. Straub, N. Y. Yip, S. Lin, J. Lee, M. Elimelech, "Harvesting Low-Grade Heat Energy Using Thermo-Osmotic Vapour Transport through Nanoporous Membranes," *Nat. Energy.*, vol. 1, pp. 16090, June 2016.

[76] S. Loeb and R. S. Norman, "Osmotic power plants," *Science,* vol. 189, pp. 654-655, 1975.

[77] K.L. Lee, R.W. Baker, H.K. Lonsdale, "Membrane for power generation by pressure retarded osmosis," *J. Membr. Sci.*, vol. 8, pp. 141-171, 1981.

[78] A Gasparatos, M. El-Haram, M. Horner, "A critical review of reductionist approaches for assessing the progress towards sustainability," *Environ. Impact Assess. Rev.,* vol. 28, pp. 286-311, June 2008.

[79] M. Aghbashlo and M. A. Rosen, "Exergoeconoenvironmental analysis as a new concept for developing thermodynamically, economically, and environmentally sound energy conversion systems," *J. Clean. Prod.*, vol. 187, pp. 190-204, June 2018.

[80] C. Bhowmik, S. Bhowmik, A. Ray, and K. M. Pandey, ''Optimal green energy planning for sustainable development: A review,'' *Renew. Sustain. Energy Rev.*, vol. 71, pp. 796–813, May 2017.

[81] World Energy Outlook, International Energy Agency; http://www.worldenergyoutlook.org-/weo2012/ [Accessed March 2016].

[82] M. R. Islam, S. Mekhilef, R. Saidur, "Progress and recent trends of wind energy technology," *Renew. Sustain. Energy Rev.,* vol. 21, pp. 456-468, Feb. 2013.

[83] S.-Y. Pan, M. Gao, K. J. Shah, J. Zheng, S.-L. Pei, P.-C. Chiang, "Establishment of enhanced geothermal energy utilization plans: Barriers and Strategies," *Renew. Ener.,* vol. 132, pp. 19-32, July 2018.\

[84] X. Song, Y. Shi, G. Li, R. Yang, G. Wang, R. Zheng, J. Li, Z. Lyu, "Numerical simulation of heat extraction performance in enhanced geothermal system with multilateral wells," Appli. Energy, vol. 218, pp. 325-337, May 2018.

[85] C. Rubio-Maya, V. M. A. Diaz, E. P. Martinez, J. M. Belman-Flores, "Cascade utilization of low and medium enthalpy geothermal resources – A review," *Renew. Sustain. Energy Rev.,* vol. 52, pp. 689-716, Dec. 2015.

[86] S. N. Aarnorsson, S. Thorhallsson, A Stefansson, "Utilization of geothermal resources," *Elsevier,* pp. 1235-1252, 2015.

[87] C. B. Field, J. E. Campbell, D. B. Lobell, "Biomass energy: the scale of the potential resource," *Trend in Ecology and Evolution,* vol. 23, pp. 65-72, Feb. 2008.

[88] W. Coyle, "The future if biofuels: a global perspective," *Amber Waves,* vol. 5, pp. 24-29, 2007.

[89] A. V. Bridgwater, "Review of fast pyrolysis of biomass and product upgrading," *Biomass Bioenergy,* vol. 38, pp. 68-94, Mar. 2012.

[90] H. Nautiyal and V. Goel, "Sustainability assessment of hydropower projects," *J. Clean. Prod.,* vol. 265, pp. 121661, Apr. 2020.

[91] K. Matsuyama, R. Makabe, T. Ueyama, H. Sakai, K. Saito, T. Okumura, H. Hayashi, A. Tanioka, "Power generation system based on pressure retarded osmosis with a commercially-available hollow fiber PRO membrane module using seawater and freshwater," *Desalination,* vol. 499, pp. 114805, Nov. 2020.

[92] H. Sakai, T. Ueyama, M. Irie, K. Matsuyama, A. Tanioka, K. Saito, A. Kumano, "Energy recovery by PRO in seawater desalination plant," *Desalination,* vol. 389, pp. 52-57, Feb. 2016.

[93] R. Makabe, T. Ueyama, H. Sakai, A. Tanioka, "Commercial Pressure Retarded Osmosis systems for Seawater Desalination Plants," *Membranes,* vol. 11, pp. 69, Jan. 2021.

[94] K. Saito, M. Irie, S. Zaitsu, H. Sakai, H. Hayashi, A. Tanioka, "Power generation with salinity gradient by pressure retarded osmosis using concentrated brine from SWRO system and treated sewage as pure water," *Desalination and water treatment,* vol. 41, pp. 114-121, 2012.

[95] A. E. Zadeh, K. Touati, C. N. Mulligan, J. R. McCutcheon, Md. S. Rahaman, "Closed-loop pressure retarded osmosis draw solutions and their regeneration processes: A review," *Renew. Sustain. Energy Rev.,* vol. 159, pp.112191, Feb. 2022.

[96] H. Q. Dang, W. E. Price, L. D. Ngheim, "The effect of feed solution temperature on pore size and trace organic contaminant rejection by nanofiltration membrane NF270," *Separation and Purification Technology,* vol. 125, pp. 43-51, Apr. 2014.

[97] L. H. Andrade, A. O. Aguiar, W. L. Pires, G. A. Miranda, M. C. S. Amaral, "Integrated ultrafiltration-nanofiltration membrane processes applied to the treatment of gold mining effluent: Influence of feed pH and temperature," *Separation Science and Technology,* vol. 52, pp. 756-766, Jan. 2017.

[98] N. Ghaffour, M. W. Naceur, N. Drouiche, H. Mahmoudi, "Use of ultrafiltration membranes in the treatment of refinery wastewaters," *Desalination and Water treatment,* vol. 5, pp. 159-166, Aug. 2012.

[99] M. R. Teixeira, M. J. Rosa, M. Nystrom, "The role of membrane charge on nanofiltration performance," *J. Membr. Sci.,* vol. 265, pp. 160-166, Nov. 2005.

[100] E. Curcio, X. Ji, A. M. Quazi, S. Barghi, G. Di Profio, E. Fontananova, T. Macleod, E. Drioli, "Hybrid nanofiltration-membrane crystallization system for the treatment of sulfate waste," *J. Membr. Sci.,* vol. 360, pp. 493-498, Sep. 2010.

[101] J. Luo, L. Ding, Y. Wan, M. Y. Jaffrin, "Threshold flux for shear-enhanced nanofiltration: experimental observation in dairy wastewater treatment," *J. Membr. Sci.,* vol. 409, pp. 276-284, 2012.

[102] M. C. S. Amaral, L. B. Grossi, R. L. Ramos, B. C. Ricci, L. H. Andrade, "Integrated UF-NF-RO route for gold mining effluent treatment: From bench-scale to pilot-scale," *Desalination,* vol. 440, pp. 111-121, Mar. 2018.

[103] N. Y. Yip and M. Elimelech, "Performance limiting effects in power generation from alinity gradients by pressure retarded osmosis," *Environ. Sci. Technol.,* vol. 45, pp. 10273-10282, Oct. 2011.

[104] K. Gerstandt, K.-V. Peinemann, S.E. Skilhagen, T. Thorsen, T. Holt, "Membrane processes in energy supply for an osmotic power plant," *Desalination*, vol. 224, pp. 64–70, Apr. 2008.

[105] D. I. Kim, J. Kim, H. K. Shon, S. Hong, "Pressure retarded osmosis (PRO) for integrating seawater desalination and wastewater reclamation: energy consumption and fouling," *J. Membr. Sci.,* vol. 483, pp. 34-41, Feb. 2015.